Naval Command,
Control and Ocean
Surveillance Center RDT&E Division San Diego, CA
92152-5001

Effect of Surface Condition on Strength and Fatigue Beha of Alumina Ceramic

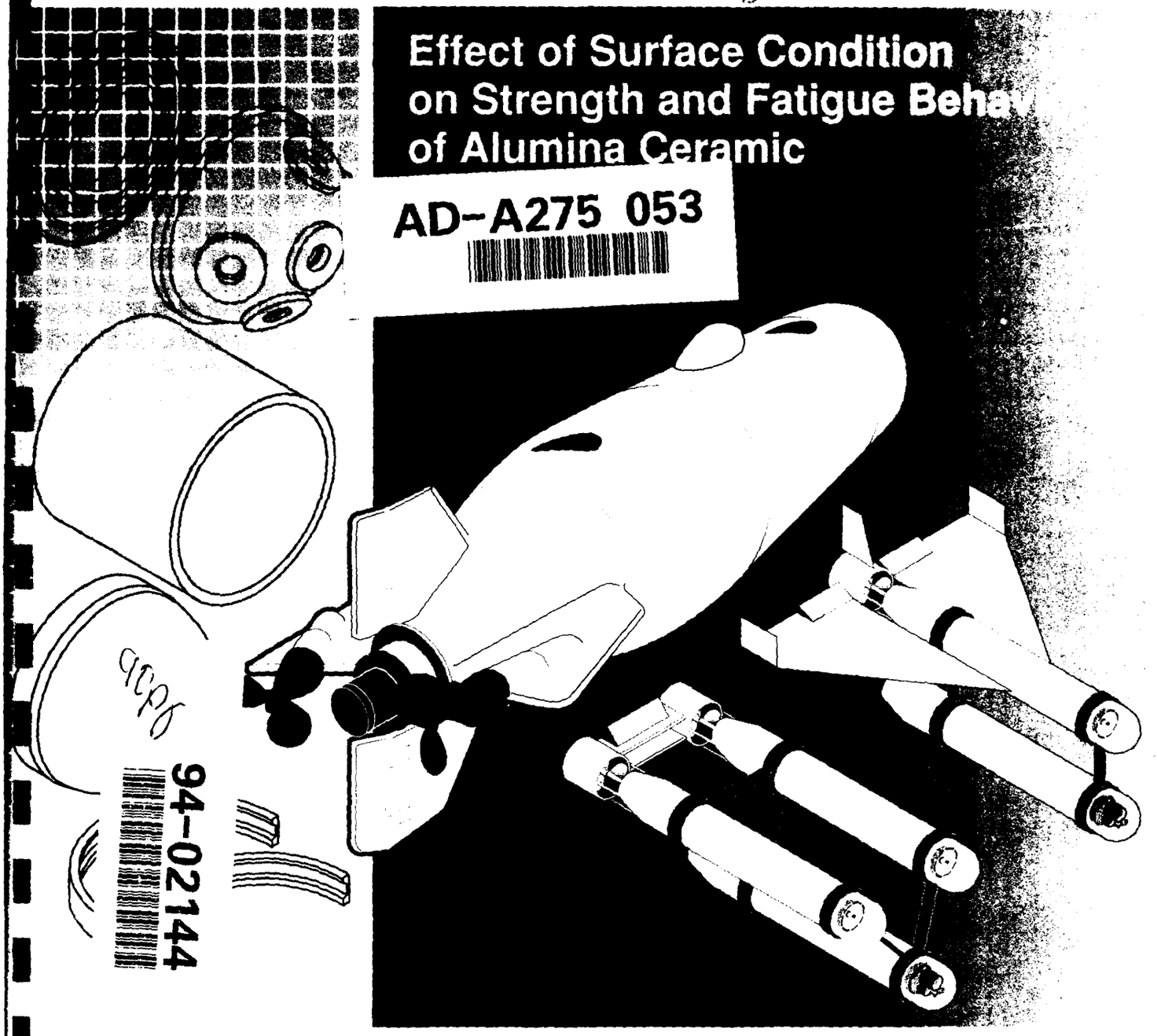

Oak Ridge
National Laboratory

Technical Document 2584
November 1993

Technical Document 2584
November 1993

Effect of Surface Condition on Strength and Fatigue Behavior of Alumina Ceramic

Oak Ridge National Laboratory

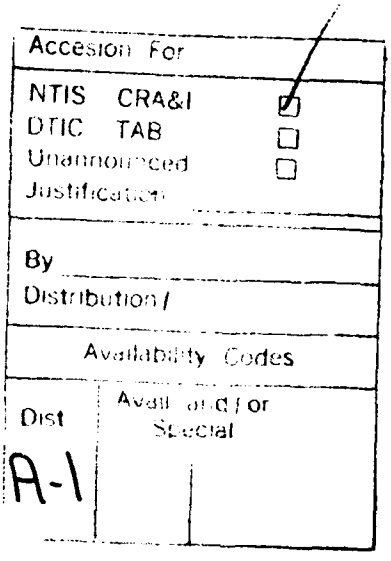

NAVAL COMMAND, CONTROL AND OCEAN SURVEILLANCE CENTER
RDT&E DIVISION
San Diego, California 92152–5001

K. E. EVANS, CAPT, USN
Commanding Officer

R. T. SHEARER
Executive Director

ADMINISTRATIVE INFORMATION

This project was performed for the Naval Sea Systems Command, Washington, DC 20362, under program element 0603713N. Contract N66001–92–M–P00120 was carried out by Oak Ridge National Laboratory, Oak Ridge, Tennessee, 37831, under the technical coordination of Ocean Technology Branch, Code 564, at the Naval Command, Control and Ocean Surveillance Center (NCCOSC), RDT&E Division, San Diego, California 92152–5001.

Released by
R. L .Wernli, Head
Ocean Technology Branch

Under authority of
N. B. Estabrook, Head
Ocean Engineering Division

LR

Table of Contents

Effect of Surface Condition on Strength and Fatigue Behavior of Alumina

A. E. Pasto, B. L. Cox, M. K. Ferber, C. R. Hubbard,
M. L. Santella, W. A. Simpson, Jr., and T. R. Watkins

Oak Ridge National Laboratory
P.O. Box 2008
Oak Ridge, Tennessee 37831

EXECUTIVE SUMMARY

The United States Navy is developing deep-water submersible vessels and, in an effort to attain the appropriate strength and buoyancy characteristics, is investigating the suitability of ceramics. The vessels typically consist of cylindrical sections and hemispherical end caps of a ceramic such as aluminum oxide (alumina), which are joined together via metallic rings made of a titanium alloy. Tests of such vessels have shown that fatigue cracks may arise in the alumina during submergence - emergence cycles, which ultimately lead to failure of the vessel. This report represents results from a one-year program designed to develop a fatigue-crack-growth resistant interface between the alumina cylinder sections and the titanium alloy rings.

The program involved two major thrusts: (1) to investigate and mitigate the effects of ceramic grinding procedures on crack generation and growth, and (2) to attempt to "heal" any damage caused by these finishing techniques. Several destructive and nondestructive examination (NDE) techniques were employed to evaluate the effects of the crack growth modification techniques. The destructive techniques included modulus of rupture (MOR), compressive strength, and compressive fatigue strength measurement, and fractographic and ceramographic examination. NDE examinations included dye penetrant and ultrasonic inspection, and X-ray residual stress measurement.

Results show that the strength of the AL-600 alumina is largely dominated by catastrophic crack growth from pre-existing pores in the alumina. Machining techniques can affect strength in two ways: by modifying the residual stress state of the surface, and by generating new fracture origins, such as subsurface cracks. Relatively severe machining (such as use of large abrasive grit wheels) causes compressive residual stresses on the surface, and this results in higher strength. The residual stress can be relieved by thermal treatment, which will return the MOR strength to its original (unperturbed) value. However, when the grinding becomes too severe, such as with very large grit sizes, the effect of a high residual compressive stress can be overcome by the generation of new, larger fracture origins, such as microcracks. Thus, strength will decrease.

Because of the pores in the alumina and their dominant effect on strength, attempts to heal the surface grinding damage result in no improvement in strength over that induced by the added residual stress. Thermal annealing relieves the compressive stress at the surface induced by the grinding, thereby reducing the MOR strength. Ion implantation with Cr^{3+} ions resulted in no improvement of strength. Chemical ion exchange of the impurity cations Mg^{2+} and Ca^{2+} in the intergranular glass by Ba^{2+} ions showed no strength improvement either.

Mechanical testing showed that this AL-600 alumina is extremely difficult to fracture in compressive fatigue at stresses similar to those used for test cylinders at NCCOSC. This may be caused by the fact that this alumina is stronger than the alumina used for the previously tested cylinders (AD-94, from Coors Ceramics Co.).

A potentially important result of this study has been the realization that the titanium contact member is an important contributor to the failure of the alumina. The interaction of this titanium with the alumina will vary depending on the alloy used and its heat treatment and finishing, such that the measured "strength" of the alumina tested in contact with it will vary.

Effect of Surface Condition on Strength and Fatigue Behavior of Alumina

A. E. Pasto, B. L. Cox, M. K. Ferber, C. R. Hubbard,
M. L. Santella, W. A. Simpson, Jr., and T. R. Watkins

Oak Ridge National Laboratory
Oak Ridge, Tennessee 37831

ABSTRACT

Results are presented from a program designed to prevent failure of machined cylindrical alumina components in cyclic compressive stress contact with titanium metal. Machined surfaces were generated by several finishing techniques, and their physical and mechanical states were assessed by nondestructive and destructive techniques. Post-finishing processes designed to prevent fatigue crack growth into the alumina were evaluated.

INTRODUCTION

The United States Navy is developing deep-water submersible vessels and, in an effort to attain the appropriate strength and buoyancy characteristics, is investigating the suitability of ceramics[1]. The vessels typically consist of cylindrical sections and hemispherical end caps of a ceramic such as aluminum oxide (alumina), which are joined together via metallic rings made of a titanium alloy. Tests of such vessels have shown that fatigue cracks may arise in the alumina during submergence - emergence cycles, which ultimately lead to failure of the vessel.[2] This report represents results from a one-year program designed to develop a fatigue-crack-growth resistant interface between the alumina cylinder sections and the titanium alloy rings.[3]

The program involved two major thrusts: (1) to investigate and mitigate the effects of ceramic grinding procedures on crack generation and growth, and (2) to attempt to "heal" any damage caused by these finishing techniques. Several destructive and nondestructive examination (NDE) techniques were employed to evaluate the effects of the crack growth modification techniques. The destructive techniques included modulus of rupture (MOR), compressive strength, and compressive fatigue strength measurement, and fractographic and ceramographic examination. NDE examinations included dye penetrant and ultrasonic inspection, and X-ray residual stress measurement.

PROCEDURES AND EQUIPMENT

MATERIALS

The alumina utilized in these tests was the same as that purchased under competitive bid by the Navy for fabrication of full-size components: Wesgo AL-600, a 96% alumina body. It is shaped by isostatic pressing, then sintered and diamond ground to specification by the manufacturer. Sixteen billets of about $2.5 \times 10 \times 25$ cm ($1 \times 4 \times 10$ in) dimension were received from Wesgo, Inc. The manufacturer's data sheet lists an aluminum oxide content of 96.0 w/o, a modulus of rupture of 365 MPa (53 ksi), a compressive strength of >2070 MPa (>300 ksi), and a bulk specific gravity of 3.72 g/cm^3.

A second alumina (Coors Ceramics Co. AD-94) was also tested, but only for mechanical strength, to serve as a baseline for comparison of the Wesgo material. The Coors test bars were cut from a 12-in.-diam cylinder which had previously been submergence-tested. Because of the possibility of fatigue crack damage having been introduced into the ends of the cylinder, the material for testing was cut from the central portion of the cylinder. MOR bars were prepared by longitudinal grinding of material oriented both parallel and perpendicular to the cylinder's longitudinal axis.

SPECIMEN PREPARATION

MOR Bars

Modulus of rupture (MOR) test specimens were sliced from the bulk and diamond ground to $3 \times 4 \times 50$ mm ($0.12 \times 0.16 \times 2.0$ in.) dimensions. Several machining procedures, described generally in Table 1, and in detail in Appendix A, were utilized to attain final dimensions. The machine used for most flexure specimens was a Harig 618 surface grinder. Residual stress specimens of dimension 30×30 mm (1.2×1.2 in.) were also machined on the same surface grinders as the MOR specimens. Procedures are described in Table 2 and Appendix A. A set of MOR specimens was machined on a Nicco creep feed grinder with COMMEC electrochemical discharge augmentation to the grinding wheel. All specimens had 45 degree chamfers to minimize edge cracking. MOR specimens were machined in the longitudinal direction.

Cylinders

Compressive strength and compressive cyclic fatigue strength specimens were 13 mm diam × 39 mm (0.5 × 1.5 in.) long right circular cylinders machined on a Jungner PSA-600 4-axis grinder. These specimens were machined in both unidirectional and circular directions on the ends. A set of cylindrical specimens was also machined on a lathe using a 75% diamond in 25% silicon carbide matrix tool (brand name Diasil). The cyclic fatigue tests were designed to simulate failures occurring during the Navy's testing of the large diameter tubes. A total of 17 cylindrical compression specimens was tested for fast fracture while a total of 15 specimens was subjected to cyclic loading. Four machining processes (Procedures 3 through 6 in Table 3 and Appendix A) were used to prepare the ends of the specimens which were actually tested. Other machining techniques were also evaluated, but the specimens were not mechanically tested.

CHARACTERIZATION

Ceramography

Specimens were mounted in standard metallographic mounts and polished. Micrographs were taken at magnifications of 50X to 400X to allow measurement of grain size and determine presence of grain boundary phases, pores, and other microstructural artifacts. Subsequently, electron probe microanalysis (JEOL Superprobe 7 Model 733) was performed on the grain boundary phase to elucidate the chemical species present.

Surface Analysis

Specimens of both the MOR bar and the cylinder, as finished via Procedure 1, were examined for surface texture at Rodenstock Inc., utilizing a laser surface profilometer. With this device, profiles of microscopic surface terrain over spans of up to 60 mm (2.4 in.) are achievable at a scan rate of 30 mm/min (1.2 in./min). The laser beam optics offer lateral spatial resolution on the order of one micron (40 μin.) and height resolution of about 10 nm, or 100Å (0.4 μin.).

The surface profilometer software calculates numerous parameters from the surface roughness profile. Numerous roughness values have been developed for characterization of machined metals; however, they have limited applicability to assessment of ceramics. The mechanical behavior of ceramics is likely dependent on the one deepest valley present, which would be a Griffith flaw (the most critical flaw under the applied stress). The roughness characteristics shown below are believed to be the most pertinent to ceramics; they are readily determined from algorithms intended for metallic surface inspection.

- Ra is the arithmetic average of deviations from the calculated mean line of the profile.

- Rq is the RMS (root mean square) value of the roughness profile.

- Sk is the skewness, a measure of the asymmetry about the mean line of the profile the third moment of the roughness data).

- Rv is the deepest valley in the scan. This value was not available from the software, which is primarily concerned with assessment of surface peaks, but was calculated given the maximum peak to valley excursion and the largest peak present in the scan.

Roughness characteristics were determined for the as-machined MOR bar and the end of a cylindrical specimen. Five longitudinal scans, 5 mm (0.2 in.) long, were obtained at random locations on the tensile surface of the specimens.

Nondestructive Examination

Ultrasonic nondestructive evaluation of several of the alumina samples was performed using a modified Panametrics HYSCAN system. The modifications included installation of a scan controller card and a 100-MHz, 8-bit digitizer board in a 80386-based personal computer system, as well as software for data acquisition and display. The system is capable of acquiring data in incremental steps as small as 12.7 μm (0.0005 in.) and at linear speeds up to about 127 mm (5 in.). Images up to 3200 × 3200 pixels can be acquired and displayed in color, black-and-white, pseudo-three dimensional, and enhanced formats.

Transducer excitation and flaw echo detection were accomplished with a Panametrics 5600-T pulser/receiver. This unit has a 100-MHz bandwidth and a total gain of 30 dB.

Inasmuch as surface and near-surface flaws were of primary interest for the NCCOSC samples, all ultrasonic evaluation was performed using 50-MHz surface acoustic waves. These waves are highly sensitive to flaws lying on or within about one wavelength (120 μm at 50 MHz) of the surface. The transducer used was a 50-MHz, f/0.8 normal incidence unit having a high numerical aperture, which produces a cone of incident rays, some of which lie at the critical angle (~14°) for surface-wave generation in alumina. This method of generation produces a radially propagating surface wave which is sensitive to

cracks having arbitrary orientation. In addition, we have demonstrated the ability of this system to detect surface pits as small as 10 μm (400 μin.) in diameter and 10 μm (400 μin.) deep.

Because the surface-wave beam diameter is about 300 μm (0.01 in.) at the sample surface, all such data were acquired on a 127-μm (0.005 in.) increment. This step size provides a high probability of detection while insuring rapid scanning of the samples. During scanning, a few indications comparable to those obtained from 10-25 μm (400-1000 μin.) flaws were detected in each sample.

Residual Stress

The machined specimens were examined using the 4-axis Scintag goniometer mated to an 18 kW MAC Science rotating anode generator. Cr radiation was used because of its shallow penetration depth (~8 μm, or 300 μin.). The power level was set at 9 kW (30 kV, 300 mA). Specimens were mounted on an oscillating head to improve counting statistics and oscillated parallel to the grinding direction. A 2-mm collimator was used with 3 and 0.3 mm (0.12 and 0.012 in., respectively) receiving slits. Seven tilt angles were employed in equal steps of $\sin^2\Psi$ (±55°). The (1·0·10) and (1·1·9) reflections of alumina were scanned at 0.02° 2Θ/step and 10 sec/point from 134 to 137.5 °2Θ. The $\sin^2\Psi$ technique was used to calculate the residual stresses assuming a biaxial stress state. Elastic modulus was assumed to be 246 GPa for the (1·0·10) and (1·1·9) directions[4]. Finally, in order to evaluate possible texture effects, rocking curve analysis was performed.

Mechanical Testing

MOR testing was used as a rapid method to assess the mechanical status of the surface. Changes in the state of residual stress and/or the nature of surface damage are readily observed. Selected finishing or post-finishing processes were applied to cylindrical specimens, and effects on compressive strength and compressive cyclic fatigue life were investigated.

All mechanical testing was performed with an electromechanical machine (Instron Model 6027) with a load capacity of 200 kN (45 kip). The test machine was configured to apply loads up to 10 kN (2245 lb) at test speeds ranging from 1 μm/min (40 μin./min) to 1000 mm/min (2.5 ft/min). It was controlled by an electronic console consisting of a microprocessor and keyboard. Data generated during testing may be displayed on an x-y recorder and/or transferred directly to a personal computer. This machine is depicted in Appendix B, Fig. B1.

MOR specimens were 3 × 4 × 50 mm (0.12 × 0.16 × 2.0 in.) rectangular bars per MIL-SPEC-1942 B, tested with four-point geometry at 20 and 40 mm (0.8 and 1.6 in.,

respectively) inner and outer spans. The fixture is depicted in Fig. B2, and its load transfer frame in Fig. B3. Compression specimens were 13 mm (0.51 in.) diam right circular cylinders of 39 mm (1.54 in.) length. Titanium loading rods interfaced between the alumina and the steel support platens on the electromechanical machine. Photographs of cylindrical specimens loaded into the machine ready for testing are shown in Figs. B1 and B4.

Figure 1 illustrates the test geometry, which involves the compression loading of a cylindrical specimen. For a given test, the Al_2O_3 compression specimen was positioned in the load train. Disposable titanium disks having the same diameter as the Al_2O_3 compression specimen were used at the load contact faces. Axial bending in the specimen was measured before each test by utilizing a clip-on strain gage which was sequentially positioned at 90° intervals around the specimen's perimeter. The specimen/disk contact faces were adjusted until bending was minimized (<8%). The specimen was then cycled in compression- compression (ratio of maximum to minimum stress = 0.1, frequency = 0.7 Hz). Tracking strain was monitored during the test via the clip-on strain gage. Data were acquired using a Macintosh computer and included test time, tracking and peak loads, number of cycles, and tracking strain.

MODIFICATION OF GROUND SURFACES

Annealing

Four MOR bars, machined using Procedure 1, were placed into pure alumina boats and heated in a C-M furnace in air to 1400°C (2550°F), held for four h, then cooled to room temperature at 50°C/h (122°F/h).

Ion Implantation

Ion implantation of Cr^{52} ions was accomplished, utilizing an accelerator in the Solid State Division at ORNL. The dose was 2×10^{17} Cr ions per cm^2 (1.29×10^{18} ions/$in.^2$) of surface, implanted at 125 keV. Four bars (machined using Procedure 1) were exposed to the approximately 1/2-in.-diam beam, two at a time. The bars are shown in Fig. 2, with the implanted region being perceptible due to the darkening caused by lattice defects in the material.

Ion Exchange

Microprobe results indicated the presence of Mg and Ca as major impurity cations in the siliceous grain boundary phase of the alumina. Therefore, cation exchange experiments were performed by submerging four MOR bars (machined using Procedure 1)

in beds of $BaCO_3$ powder contained in alumina crucibles and heating to 900°C (1650°F) with a 4 h hold. The residual carbonate on the bars was removed by light abrasion after several days exposure to laboratory atmosphere.

RESULTS

CERAMOGRAPHY

A micrograph of the AL-600 alumina as machined using Procedure 1 is presented in Fig. 3. Two specimens were mounted with their machined faces parallel to each other and with these faces perpendicular to the surface of the mount. Accordingly, the region of interest to the current study is that near the bar-mount interface. No cracking can be observed here, nor is there any indication of a high density of large defects. A large amount of pullout damage was incurred during the polishing, and it manifests itself as the darkest areas. Some rounded dark areas are present: these are pores. This is a relatively coarse grained alumina, with grains of tens of microns linear dimension, as observed in the higher magnification back-scattered electron microprobe photograph [Fig. 4(a)].

No other materials were examined by this ceramographic technique, since the bars shown here were machined by a "rough" technique (120 grit wheel) and ceramography was not able to show any machining-induced defects, such as cracks.

Electron probe microanalysis reveals the presence of major amounts of silicon in the grain boundary phase [Fig. 4(b)], along with minor amounts of Mg and Ca [Figs. 4(c) and 4(d), respectively]. No other impurities were detected by this method.

SURFACE ANALYSIS

Specimens of both the MOR bar and the cylinder, as finished via Procedures 1 and 3, respectively, were examined for surface texture at Rodenstock Inc., utilizing a laser surface profilometer. The averages for the roughness characteristics for the two materials are shown in Table 4. Grinding grooves on the longitudinal section of the MOR bars were plainly evident as a modulation of the surface profile (Fig. 5), and the roughness was evident as an overlay to the profile (Fig. 6). Average roughness was 2.24 μm (88 μin.) which is considered a very rough finish for structural ceramics ("good" finishes are 2-8 μin., or 0.05 to 0.2 μm). The cylinder end, which was finished by the same grit wheel, showed identical surface roughness (2.25 μm), but a much different waviness, or texture (Fig. 7). This different texture arises from the nature of the motion of the wheel relative to the workpiece. For MOR bars, a rotating wheel is fed into a stationary bar, leaving unidirectional grinding grooves. For the cylinder, a side face of a rotating wheel is fed into

the counter rotating end of the cylinder. This difference is also noted in the ultrasonic NDE examination, described below. One major difference detected was in the skewness parameter, which indicates the relative amount of the surface roughness due to "valleys" in the material induced by the grinding. The MOR bar exhibited a skewness value of -0.33, whereas the cylinder end measured -0.52. In previous work[5] on machining, involving silicon nitride structural ceramics, differences of this magnitude correlated strongly to strength differences.

NONDESTRUCTIVE EXAMINATION

Ten alumina MOR bars (machined using Procedure 1) and one cylindrical specimen (machined by Procedure 4) were evaluated ultrasonically. Since the major concern with these samples is surface quality and the detection of surface and near-surface machining damage, the primary method of inspection was a high-frequency surface acoustic wave. This test is extremely sensitive to defects on or within one wavelength of the surface; thus, at the inspection frequency of 50 MHz, defects lying on or within about 120 μm (0.005 in.) of the surface should be imaged. The ability to detect surface flaws as small as 10 μm (0.0004 in.) with this approach has been previously demonstrated.

Figure 8 shows the results obtained on the top surface of the ten MOR bars. The bars are numbered 1 to 10 from top to bottom. The gray scale to the right of th figure depicts the amplitude of the ultrasonic surface wave, with lighter shades representing greater surface-wave amplitude. The linear features running horizontally along each bar are very fine (ca.10 μm, or 0.0004 in.) grinding marks. The few dark, pointlike indications seen on some of the bars (most notably the right end of bars 1 and 2), are surface or subsurface flaws, probably voids in the 20-40 μm (0.0008 - 0.0016 in.) range. It is important to note that, while some flaws can be detected in the samples, this material is easily the highest quality monolithic alumina examined in this laboratory, in terms of uniformity, high density, and freedom from NDE-detectable flaws.

Although it is not routine to inspect samples for volumetric flaws, the high quality of the ceramic made it worthwhile to examine this initial batch of MOR bars for flaws throughout the sample thickness. Accordingly, the samples were inspected with a 75-MHz, focused transducer. The transducer was focused near the midplane of the sample, but the response is within 6 dB of maximum for about 6 wavelengths above and 3 wavelengths below focus. This asymmetry makes it desirable to scan the samples from both sides to maximize the coverage. Figure 9 shows the results obtained from the top surface. The gray scale has been inverted to make the flaws (the dark, pointlike indications) more obvious. These flaws are not those detected in the surface-wave

inspection; the volumetric flaw test is "blind" to defects on or within about 200 μm (0.008 in.) of the surface. As before, the volumetric results indicate that the material is very homogeneous with high density.

Figure 10(a) shows the surface-wave results obtained on the top surface of the cylindrical specimen. The approximately radial lines are grinding marks, which can be detected visually. The most distinctive feature is the seashell-shaped structure in the upper half of the figure. This feature can also be detected visually and was apparently produced during grinding. The dark, pointlike indication near the top center of the figure is a subsurface flaw.

Figure 10(b) shows the surface-wave results from the bottom surface of the cylinder. As before, the radial (or arclike) lines are grinding marks. However, the very dark indication at about the ten o'clock position on the figure is a pit or surface pullout (i.e., an area in which a crystal or several grains are pulled out of the surface). This region is about 150 μm long × 75-100 μm wide × 50 μm deep (0.006 × 0.003-0.004 × 0.002 in.), as measured by light microscopy. Visually, it has a very rough interior surface, as though the sample had been fractured and the affected material pulled out during grinding.

A second AL-600 cylinder was subjected to nondestructive evaluation. This specimen was ground unidirectionally (Procedure 6), which, of course, produces linear grinding marks rather than the "scalloped" marks characteristic of the first cylinder examined (Procedure 4) . As before, the ends of the cylinder were examined using a 50-MHz, radially propagating surface wave. The transducer height (i.e., transducer-to-specimen distance) was adjusted to produce a beam diameter on the sample of about 300 μm (0.012 in.). This, in turn, produces a surface-wave delay of about 50 nsec with respect to the specularly reflected signal from the beam entry surface.

Figure 11(a) shows the results obtained on the cylinder top surface and Figure 11(b) those on the bottom surface. The dark linear indications are grinding marks, which appear to be more intense than those detected on the first cylinder examined. However, the only evidence of surface or subsurface flaws found was the faint, pointlike indication near the three o'clock edge position in Figure 11(b). This feature, for which no surface flaw could be found using visual microscopy, probably originates from a very small subsurface void.

RESIDUAL STRESS

The specimens showed modest non-random/non-uniform texture, with polefigures showing maximum intensity difference of about 2X. Further, rocking curves indicated that the material contained large grains, at least greater than about 5 μm (0.0002 in.), a fact

which was shown by the ceramography. Origins of the non-uniformity could include (1) large or coarse grain size, or (2) hard agglomerates with preferred orientation.

Table 5 lists all the residual stresses measured in this study to date. Compressive residual stresses were observed with these specimens, as follows:

- as the abrasive particle size of the final finishing step increased, the compressive residual stress increased (compare residual stress plates, Procedures 2 and 2A to Procedure 1),

- residual stresses perpendicular to the grinding direction were about 2X those parallel to the grinding direction, as has been observed in other studies,[6-7]

- residual stress appeared to be independent of location within the plate "interior" and was reproducible,

- residual stress in the plates was approximately equal to that in bars (compare ion-implanted MOR Bar machined with Procedure 1 to the residual stress plate machined with Procedure 1),

- residual stresses were effectively equivalent for materials finished with 320 grit abrasive, regardless of whether or not there was an intermediate step utilizing an intermediate sized grit (Procedures 2 and 2A),

- residual stresses were effectively equivalent for 240 grit and 320 grit machined specimens.

The compressive residual stresses measured here were less than those reported elsewhere[8-9] for similar materials. This discrepancy may be due to the lack of sensitivity of the measurement to very shallow residual stresses. In other words, because the depth of ion-implantation was small (~80 nm, or 30 μin.) relative to the penetration depth of the X-rays (~8 μm, or 300 μin.), the measurement provided an "average" residual stress due to ion-implantation, and grinding stresses were intermediate in magnitude.

EFFECT OF SURFACE GRINDING ON STRENGTH AND FATIGUE LIFE

Flexural Strength

The fracture strength of AL-600 flexure specimens prepared by several machining procedures was measured. For a given procedure, 20 flexure specimens were loaded to

failure at 0.5 mm/min (0.02 in./min) in the universal testing machine. Averaged results are presented in Table 6, with complete individual results detailed in Appendix B. Figure 12 illustrates the Weibull plots (fracture probability versus strength) obtained for these tests. For Procedure 1, which utilized a 120 grit wheel, the average strength was 358 MPa (51.9 ksi) with a standard deviation of 21 MPa (3 ksi). It is interesting that grinding with the finer grit (Procedure 2) actually resulted in a reduction in the average strength to 320 ± 32 MPa (46.4 ± 4.6 ksi). This behavior might be attributed to either a decrease in the residual stress generated or an increase in the level of subsurface damage generated during grinding with the 320 grit wheel. Similar trends in strength have been observed for Al_2O_3 flexure specimens which were lapped. The average strength for the specimens machined using Procedure 7 was the lowest of the three sets (304 ±16.9 MPa, or 44.0 ± 2.45 ksi), likely due to the use of the coarse 120-grit wheel in combination with the high in-feed rate (0.002 in/pass versus 0.0005 in/pass for Procedure 1).

While the Weibull modulus (m) was also reduced from 20 for Procedure 1, to 12 for Procedure 2, it was nearly unchanged for Procedure 7 specimens (21.4). As indicated in Fig. 12, the low "m" value resulting from Procedure 2 machining may have been due to the low strength tail in the distribution. In this case, the flaws associated with the low strength regime were more adversely affected by the grinding. If one were to ignore this low strength tail, then all three specimen sets would exhibit similar Weibull values.

The results displayed on Fig. 12 indicate that the distributions of flaws in the three specimen sets were quite similar. The main affect of modifying the machining process was to change the characteristic strength (i.e., the horizontal position of the Weibull graph). Scanning electron microscopy (SEM) of the fracture surfaces (Fig. 13) showed that intrinsic pores near the surface were the critical defects in nearly all of the specimens. Therefore, the surface flaws generated in the three machining processes were not of sufficient size to control failure. The most plausible explanation for the influence of machining upon the average strength is that the residual stresses were modified by the machining process. Changes in the residual stress level in the vicinity of the intrinsic pores would be expected to change the applied stress required for catastrophic failure.

The Coors material (Table 6) was somewhat weaker, exhibiting a strength of about 300 MPa (43.5 ksi) An apparent difference in strength was noted for specimens cut from the longitudinal and the circumferential directions. It was machined using Procedure 2.

Compressive Strength and Fatigue Resistance

A major challenge for the program was development of procedures to simulate the in-service compression failures observed for this material. Initially, compressive strength tests alone were performed. After an acceptable failure stress was determined, cyclic fatigue testing was performed at some lower stress level. Initial compression tests

indicated that a ceramic failure could be generated by cracking, at about 1.1 GPa (160 ksi) stress level. However, it was noted that the Ti load block appeared to have been deformed, which is plausible since unannealed Ti yields at stresses below that.

To address this yielding problem, a special thermal hardening treatment was applied to the titanium disks to increase their yield point. During subsequent cycle-to-failure tests at 828 MPa (120 ksi), failure occurred during the first cycle. As discussed below, load-to-failure compression tests conducted with the modified titanium indicated that the fracture stress was significantly lower when the modified titanium disks were used.

To assess the ultimate strength of the compression specimens, load-to-failure tests were conducted using cylindrical specimens machined using Procedures 3, 4, 5, and 6. As indicated in Table 3, these procedures involved variations on the machining steps required for preparation of the specimen ends. A minimum of two specimens from each machining procedure was fractured by loading at a displacement rate of 1.0 mm/min (0.04 in./min). In all cases but one, the specimens were tested using the as-fabricated titanium disks while the hardened titanium disks were used to fracture one set of specimens machined using Procedure 3. As shown in Fig. 14, the fracture strengths did not vary significantly with machining procedure. However, the use of the hardened titanium disks resulted in a substantial reduction in strength. This difference may have been due to an increase in the surface roughness of the hardened disks. To address this possibility, several disks were given various surface treatments (Table 7).

The use of these titanium disks resulted in substantial variations in the ultimate strength (Fig. 15). Microstructural observations of the Ti disks indicated that their surface condition was the dominating factor in controlling strength. For example, a low strength was obtained for the alumina when the Ti surface roughness was high (disks designated as A-annealed and A-annealed/cleaned). In this case, the surface asperities along the Ti disks apparently acted as stress concentrators resulting in crack initiation in the aluminum oxide specimens at relatively low applied stresses. Hardness of the Ti was also varied by the annealing process, but, as shown in Fig. 16, failure stress of the alumina did not correlate with Ti hardness.

For the cyclic fatigue studies, a triangular waveform with $f = 0.7$ Hz and $R = 0.1$ (ratio of minimum to maximum stress) was applied to all the cylindrical specimens. As shown in Fig. 17, specimen failures were only obtained for peak stresses at or above 900 MPa (130 ksi). Because 900 MPa is above the yield point of the titanium, it is likely that time-dependent deformation of the titanium was responsible for the observed failures at 900 MPa. Such deformation would induce lateral tensile stresses in the ends of the Al_2O_3 compression specimens. It is interesting that although specimen failure did not occur for the specimen cycled at a peak stress of 828 MPa (120 ksi), small cracks were observed in the specimen ends. This would be expected since 828 MPa is very near the reported yield point for the titanium. All specimens not failing were interrupted after 100,000 to 500,000

cycles. Most of these specimens were unloaded and then archived (downward arrows in Fig. 17). A few of the specimens not failing were loaded to failure (upward arrows in Fig. 17). Note that the data in this figure represents specimens prepared by different grinding procedures since grinding procedure did not influence compressive strength. Therefore, it was not expected to influence the cyclic fatigue lifetime. As shown in Fig. 18, the residual strengths for these specimens were nearly identical to the average fast fracture value reported in Fig. 14 indicating that no time-dependent weakening had occurred during load cycling.

Modification Of Ground Surfaces

Thermal annealing to remove residual stresses and to "blunt" the microcracks, if they exist, was performed. MOR test results (Table 6) show that strength was reduced by this process, by nearly 50 MPa compared to unannealed specimens. This strength reduction is nearly the same as the magnitude of the compressive residual stress measured in the surface (Table 5), implying that thermal annealing has removed the residual stress.

Ion implantation of Cr^{52} ions was accomplished as previously described. MOR test results (Table 6) show that no strength benefit was obtained by this process. The small number of data lend less significance to this conclusion than one would like, although the scatter was very small.

Ion exchange experiments on three alumina test specimens were accomplished as described earlier. MOR test results (Table 6) show that no strength benefit was obtained by this process, and it is likely, but not significantly certain given the small amount of data available, that in fact the strength is decreased.

SUMMARY

Results show that the strength of the AL-600 alumina is largely dominated by catastrophic crack growth from pre-existing pores in the alumina. Machining techniques can affect strength in two ways: by modifying the residual stress state of the surface, as is shown by the data of Table 5, and by generating new fracture origins, such as subsurface cracks. The effect of residual stress on the MOR strength of the alumina is shown in Fig. 19, using data from Tables 5 and 6. More severe machining (such as use of rougher grit wheels and/or higher infeed rates) causes more residual stress, and results in higher strength. Optimum strength results are obtained when the material is ground using Procedure 1, (e.g., that utilizing the relatively rough 120 grit wheel at a nominal 0.0005 in/pass infeed rate). This residual stress can be relieved by thermal treatment, which decreases the MOR strength. However, when the grinding becomes too severe, such as with very large grit sizes or high infeed rates as used in Procedure 7, the effect of a high

residual compressive stress can be overcome by the generation of new, larger fracture origins, such as microcracks. Thus, strength is expected to decrease, as illustrated schematically in Fig. 20.

Because of the pores in the alumina and their dominant effect on strength, attempts to heal the surface grinding damage result in no improvement in strength over that induced by the added residual stress. Thermal annealing relieves the compressive stress at the surface induced by the grinding, thereby reducing the MOR strength. Ion implantation with Cr^{3+} ions results in no improvement of strength. Chemical ion exchange of the impurity cations $Mg^{2+}$and Ca^{2+} in the intergranular glass by Ba^{2+} ions shows no strength improvement either.

Mechanical testing has shown that this AL-600 alumina is extremely difficult to fracture in compressive fatigue at stresses similar to those used for test cylinders at NCCOSC. This may be caused by the fact that this alumina is stronger than the alumina used for the previously tested cylinders (made by Coors).

Further, this study has shown that the compressive strength and compressive fatigue behavior of this AL-600 alumina are independent of machining technique. This finding is only true because of the testing procedure, involving a deformable Ti insert facing the alumina specimen ends. Ordinarily, one would expect that machining procedure would have an affect on fatigue crack initiation and growth. However, in the present case the Ti deforms during testing, placing the alumina surface in tension and causing brittle failure.

A potentially important result of this study has been the realization that the titanium contact member is an important contributor to the failure of the alumina. The interaction of this titanium with the alumina will vary depending on the alloy used and its heat treatment and finishing, such that the measured "strength" of the alumina tested in contact with it will vary.

RECOMMENDATIONS

The experimental results described above have demonstrated some important effects of surface preparation techniques for alumina and titanium on the mechanical behavior of the alumina in contact with the titanium. Recommendations follow in three areas: first, on the grinding process recommended for AL-600 alumina cylinder ends; second, on the selection of a material suitable for undersea vessel application; and third, on the needs for further work based on the present study.

First, based on the work described herein, we recommend a grinding process for the AL-600 cylinder ends to be similar to Procedure 1, inasmuch as this process yielded the greatest MOR strength. The procedure utilizes a 120 grit diamond grinding wheel, applied with an infeed rate of about 0.0005 in./pass. Roughing can be accomplished with a coarser grit wheel, such as 100 grit, and larger amounts of material can be removed per pass. See

the Procedure 1 description in Appendix A. Other alumina-based materials should behave similarly, but other materials, such as silicon nitride or boron carbide-aluminum composites, may not.

Second, regarding the selection of a material suitable for undersea vessel application, there are many factors to consider. Given a low density and high compressive strength, one material would be considered more suitable than another if it satisfies the criteria of possessing high fracture toughness; homogeneity of microstructure, composition, and thus properties; and high resistance to slow crack growth (SCG) under immersion in sea water. Aluminas containing significant amounts of grain boundary glassy phases, such as Wesgo AL-600 and Coors AD-94, are very homogeneous in terms of microstructure and properties, but have relatively low fracture toughness and thus low strength compared to e.g.- silicon nitride (K_{1c} of 3-4 vs >6, and MOR of 350 MPa vs >1000 MPa for aluminas and silicon nitrides, respectively). Further, their resistance to slow crack growth under sea water is suspect because of the known effects of water on SCG in glasses. Accordingly, one would expect that there would be many more suitable materials than these aluminas for the intended application.

However, much further work is required before a complete understanding is obtained of the nature of the fatigue cracking of alumina or other materials. Specifically, the following efforts are recommended.

1. Determination of an effective means of simulating in the laboratory the type of fatigue failure observed for cylindrical test vessels. The laboratory set-up used in this program does not contain the epoxy layer, nor does it constrain the Ti in exactly the same way as does the actual submergence testing.

2. Determination of a correlation, if it exists, between the MOR strength of the material and its fatigue behavior.

3. Completion of the mechanical testing of the alumina materials prepared by the advanced machining procedures, both as MOR bars and compressive fatigue test components.

4. Characterization of the materials, both Ti and alumina, prepared by the various surface preparation techniques. This should include not only the currently practiced ceramography, surface roughness, and ultrasonic NDE, but also evaluation or develoment of better techniques to analyze "subsurface" damage". New techniques are becoming available, such as measurement of laser scattering from subsurface cracks, or precision heat flow determination using surface scanning heaters.

REFERENCES

1. R. P Johnson, R. R. Kurkchubasche, and J. D. Stachiw, "Design and Structural Analysis of Alumina Ceramic Housings for Deep Submergence Service: Fifth Generation Housings," NCCOSC RDT&E Division TR 1583 (1993).

2. J. D. Stachiw, R. P. Johnson, and R. R. Kurkchubasche, "Evaluation of Model Scale Ceramic Housing for Deep Submergence Service: Fifth Generation", NCCOSC RDT&E Division TR 1582 (1993).

3. R. R. Kurkchubasche, R. P. Johnson, and J. D. Stachiw, "Application of Ceramics to Large Housings for Underwater Vehicles: Program Outline", NCCOSC RDT&E Division TR 1595 (1993).

4. F. F. Lange, M. R. James, and D. J. Green, "Determination of Residual Surface Stresses Caused by Grinding in Polycrystalline Al2O3," *J. Am. Ceram. Soc.*, 65 [2] C16-7 (1983).

5. A. E. Pasto and S. Natansohn, "Development of Improved Processing Methods for High Reliability Structural Ceramics for Advanced Heat Engines", ORNL/Sub/89-SD548/1, July 1992.

6. D. Johnson-Walls, A. G. Evans, D. B. Marshall, and M. R. James, "Residual Stresses in Machined Ceramic Surfaces," *J. Am. Ceram. Soc.*, 69 [1] 44-47 (1986).

7. G. A. Johnson, "Generating Compressive Residual Stress by CBN Grinding," pp. 157-67 in Residual Stress in Design, Process and Materials Selection. Edited by W. B. Young, ASM International (1987).

8. E. D. Specht, C. J. Sparks, and C. J. McHargue, "Determination of Residual Stress in Cr-Implanted Al2O3 by Glancing Angle X-Ray Diffraction," *Appl. Phys. Lett.*, 60 [18] 2216-8 (1992).

9. C. J. McHargue, M. E. O'Hern, C. W. White, and M. B. Lewis, "Ion Implantation in Ceramics-Residual Stress and Properties," *Mat. Sci. Eng.*, A115 361-7 (1989).

Table 1. Description of Flexural Test Specimen Machining Procedures.

Procedure Number	Procedure Description[a]						Materials Produced
	Slice Billet	Grind Width	Slice Length	Slice Height	Grind Height	Chamfer	
1	100/0.0005	320/0.0002	100/0.003	100/0.003	120/0.0005	240/0.005	Series 1B
1C[b]	100/0.0005	120/0.0002	100/0.003	100/0.003	120/0.0002	- - - - - - - - -	Series 3B
7	100/0.0005	120/0.002	100/0.003	100/0.002	120/0.002	120/0.005	Series 7B
2	100/0.0005	320/0.0002	100/0.003	100/0.003	320/0.0005	320/0.005	Series 2B, 5A
2	100/0.0005	320/0.0002	100/0.003	100/0.003	320/0.0005	- - - - - - - - -	Series 4A
2	100/0.0005	320/0.0005	100/0.003	100/0.003	320/0.0005	- - - - - - - - -	Series 4B
8	100/0.0005	320/0.0002	100/0.003	100/0.003	240/0.0005	240/0.005	Series 3A
2	100/0.001	320/0.0005	100/0.001	100/0.001	320/0.0005	220/belt	Coors Mat'l.

(a) Table lists abrasive grit size/wheel infeed rate or machine downfeed rate.

(b) "C" in the procedure number indicates the material was machined transversely. All others were machined longitudinally.

Table 2. Description of Residual Stress Test Specimen Machining Procedures.

Procedure No.	Procedure Description[a]				Mat'l's Prep'd
	Slice Billet	Grind Edges	Grind Surface	Finish Surfaces	
1	100/0.0005	320/0.0002	120/0.002	----------	Plate 1A1 (Side 1)
2A	100/0.0005	320/0.0002	120/0.002	320/0.0005	Plate 1A1 (Side 2)
2	100/0.0005	320/0.0005	320/0.0005	----------	Plate 7A2
9	100/0.0005	320/0.0002	---------	----------	Plate 1A

(a) Table lists abrasive grit size/wheel infeed rate or machine downfeed rate.

Table 3. Description of Cylindrical Specimen Machining Procedures.

Procedure Number	Procedure Description[a]							
	Slice Billet	Rough OD	Finish OD	Rough Length	Finish Length		Chamfer	Materials Produced
10	100/0.0005	320/0.0002	80/0.0002	100/0.001	150/0.001	[O][b]	---------	3-9 to 3-14 5-8 to 5-10 6-12, 7-12 to 7-13
3	100/0.0005	320/0.0002	320/0.0002	100/0.001	230/0.001	[O]	320/0.0002	3-1, 4-1 to 4-6 6-1 to 6-8 7-1 to 7-4 8-1 to 8-10
4	100/0.0005	320/0.0002	320/0.0002	100/0.001	320/0.001	[O]	320/0.0002	2-1 to 2-2 3-6 to 3-8 5-4 to 5-7 6-5,-9,-10,-11 7-10,-11, 8-15
6	100/0.0005	320/0.0002	320/0.0002	100/0.001	320/0.0002	[U]	320/0.0002	0-0, 3-2 to 3-5 4-7 to 4-10 5-2,-3,-11 6-7,-8, CL-1 7-8 to 7-9, 7-13 8-11 to 8-14

Table 3. Description of Cylindrical Specimen Machining Procedures. [Continued]

Procedure Number	Slice Billet	Procedure Description: Rough OD	Finish OD	Rough Length	Finish Length	Chamfer	Materials Produced
11	100/0.0005	320/0.0002	12μ/0.0002	100/0.001	12μ/0.0001[U]	12μ/0.0002	1-1 to 1-8 2-5 to 2-10
12	100/0.0005	320/0.0002	320/0.0002	100/0.001	100/0.0005[U]		4-11 to 4-16
5	100/0.0005	320/0.0002	Diasil tool[c]	100/0.003	Dia/0.001	[O] Dia/0.001	2-3 to 2-4 4-7 to 4-8 5-1,-12 7-5 to 7-6 8-16 to 8-17

(a) Table lists abrasive grit size/wheel infeed rate or machine downfeed rate.

(b) [O] indicates omnidirectional finish obtained. [U] indicates unidirectional finish obtained.

(c) Diasil tool is small button-shaped tool of diamond crystals in an SiC matirx.

Table 4. Surface Profilometry Results for an MOR bar and a Cylinder End Face

Material	Grinding Procedure	Parameter		
		R_a(μm)[μin]	R_{max}(μm)[μin]	S_k
MOR bar surface	1	2.24 [88.1]	19.4 [763]	-0.33
Cylinder end face	3	2.25 [88.5]	25.5 [1003]	-0.52

Table 5. Residual Stresses in Machined AL-600 Alumina.

Sample	Grinding Procedure	Orientation of Stress Relative to Grinding Direction	Residual Stress (MPa)[ksi]¥ Reflections (1.0.10)	(1.1.9)	Average Residual Stress (MPa)
Resid. Stress Plate #1A1 , Area #1 (120 grit wheel)	1	perpendicular	-129[18.7]	-101[14.6]	-111[16]
		parallel	-75[10.9]	-2[0.3]	-44[6.4]
Resid. Stress Plate #1A1, Area #2	1	perpendicular	-120[17.4]	-97[14.2]	
		parallel	-37[5.4]	-8[1.2]	
Resid. Stress Plate #1A1, Area #3	1	perpendicular	-111[16.2]	-120[17.4]	
		parallel	-35[5.1]	-60[8.7]	
Resid. Stress Plate #1A1, Area #3 repeat	1	perpendicular	-114[16.5]	-99[14.4]	
		parallel	-67[9.7]	-65[9.4]	
Resid. Stress Plate #1A1 (320 grit side)	2A	perpendicular	-46[6.7]	-24[3.5]	-35[5.1]
		parallel	-62[9.0]	-42[6.1]	-52[7.5]
Resid. Stress Plate #7A2 (320 grit)	2	perpendicular	-42[6.1]	-4[0.6]	-23[3.3]
		parallel	-10[1.5]	-29[4.2]	-20[2.9]
MOR Bar #3A1 (240 grit)	8	perpendicular	-33[4.8]	-49[7.1]	-41[5.9]
		parallel	-52[7.5]	-39[5.7]	-46[6.7]
Ion-Implanted MOR Bar (120 grit)	1	perpendicular	-129[18.7]	-117[17.0]	-123[18]
		parallel	-84[12.2]	-10[1.5]	-47[6.8]

¥ E/(1+n)=246 GPa (E=310 GPa, n=0.26) for the 1.1.9 reflection[5] and the 1.0.10 reflection.

Table 6. MOR Results for Alumina Test Specimens

Material + Condition	Number of Bars	Average MOR (MPa)[ksi]	Standard Dev.(MPa)[ksi]	Weibull Modulus
Wesgo AL-600				
Procedure #1	20	358 [51.9]	21 [3.0]	20
Annealed 1400°/2h	5	308 [44.7]	15 [2.2]	N/A
Cr Ion Implanted	3	353 [51.2]	3 [0.4]	N/A
Ba Ion Exchanged	3	326 [47.3]	36 [5.2]	N/A
Procedure #2	20	320 [46.4]	32 [4.6]	12
Procedure #7	20	304 [44.1]	17 [2.5]	21
COORS AD-94				
Procedure #1				
Parallel to axis	19	306 [44.4]	11 [1.6]	33
Perpendicular	5	282 [40.9]	12 [1.7]	N/A

Table 7. Designations for the Ti Disks Used for Loading the Cylindrical Test Specimens.

Designator	Batch*	Cutting Method
A-ar	1	Conventional
A-annealed**	1	Conventional
A-annealed/cleaned	1	Conventional
A-annealed/polished	1	Conventional
B-ar	2	EDM

*Batch refers to the lot of Ti disks obtained from the machine shop. Specimens in the first batch were cut using an abrasive saw and then the surfaces were ground. Batch 2 specimens were cut from the rod stock by electro-discharged machining (EDM). Nothing was done to the surfaces.

**Annealed 960°C (1760°F)/1 h; water quenched then aged 750°C (1382°F)/4 h; air-cooled.

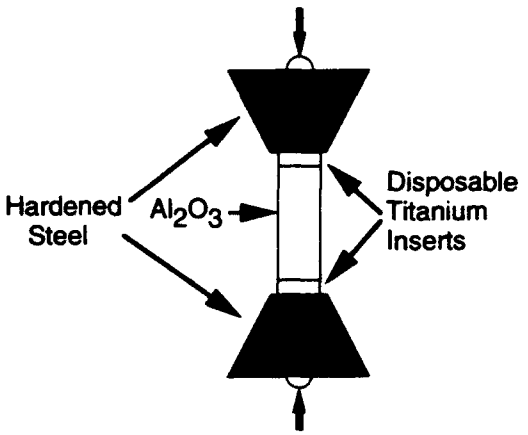

Figure 1. Schematic diagram of the compressive strength and fatigue loading arrangement.

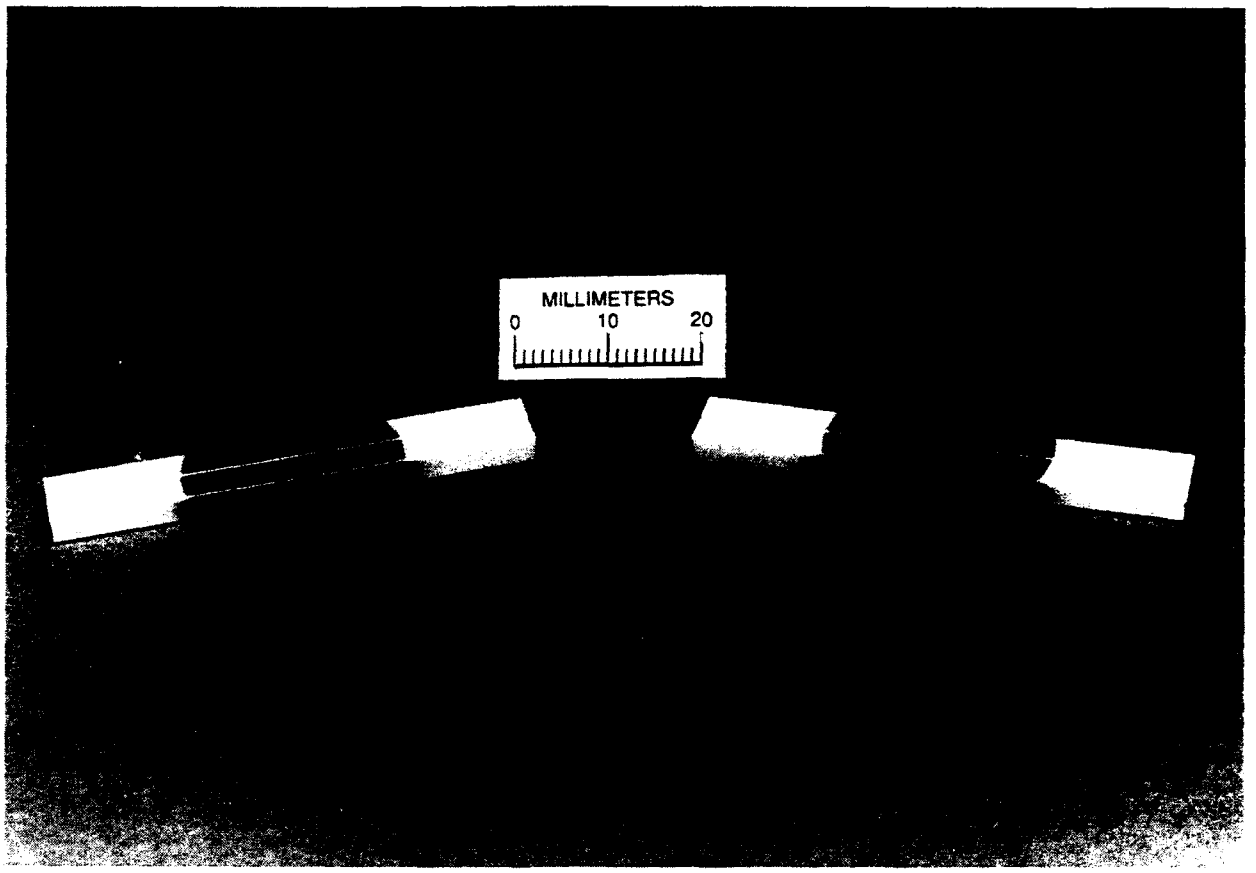

Figure 2. Four alumina MOR bars which have been ion-beam irradiated with125 keV Cr^{52} ions.

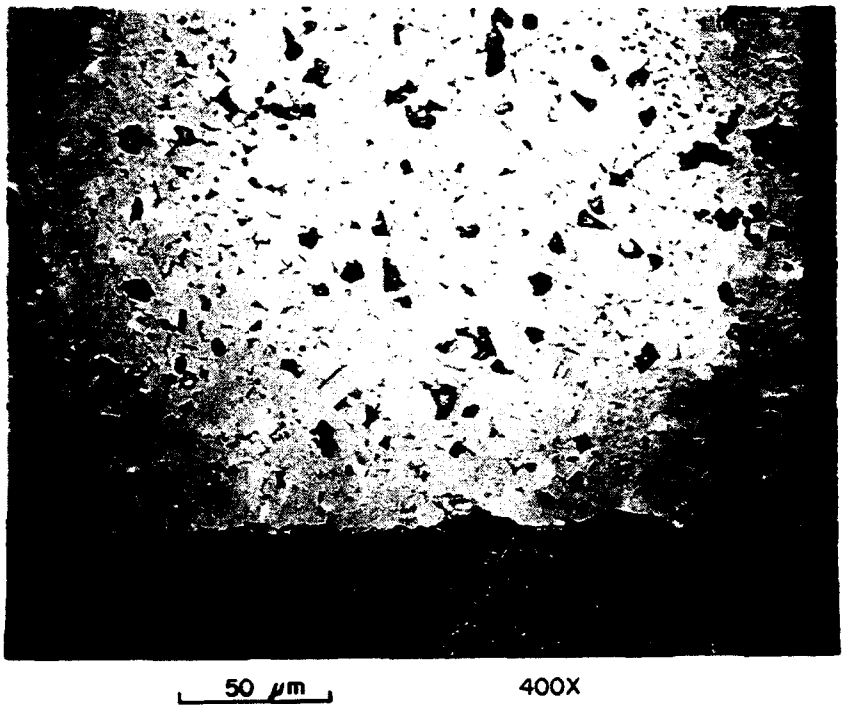

Figure 3. Optical micrograph of polished AL-600 MOR bar, on edge. Bar equals 50 µm (0.002 in). Light gray area is alumina grain, darker areas are pores (rounded) or pullouts from polishing (irregular spots).

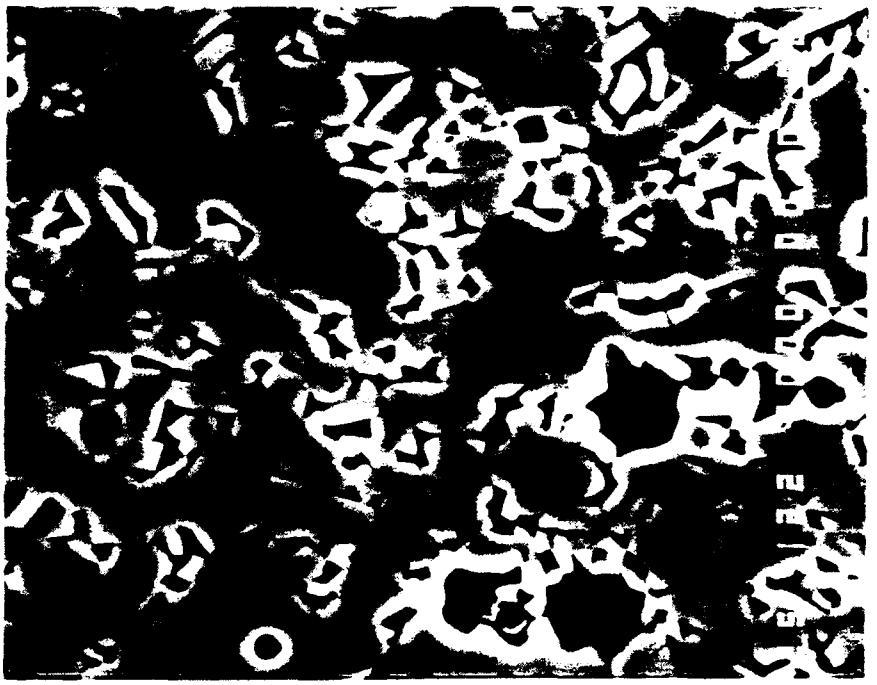

(a)

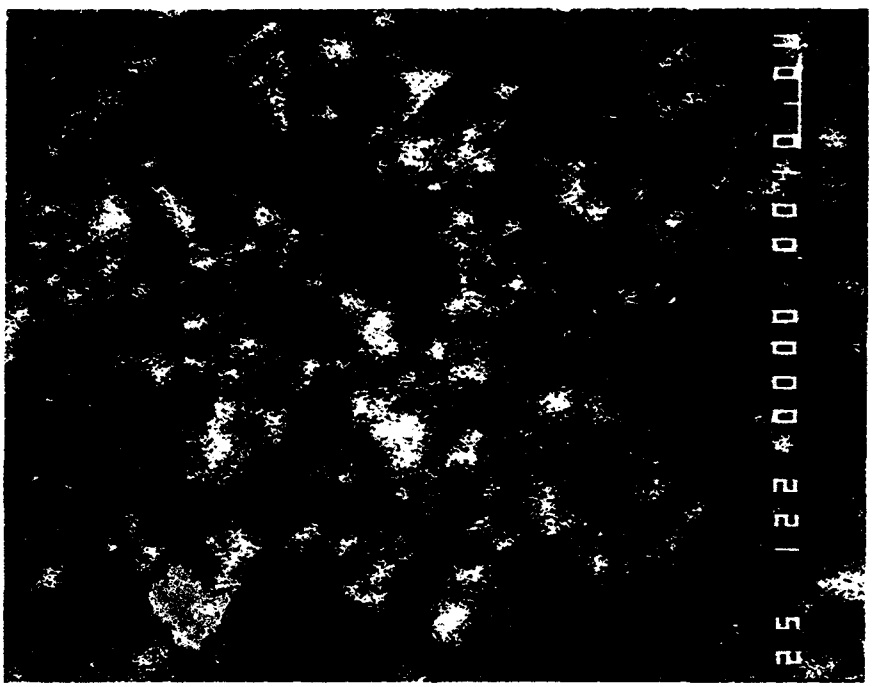

(b)

Figure 4. Back-scattered electron micrograph (a) of WESGO AL-600 alumina, with corresponding x-ray dot map for Si, showing siliceouus grain boundary phase distribution (b).

(c)

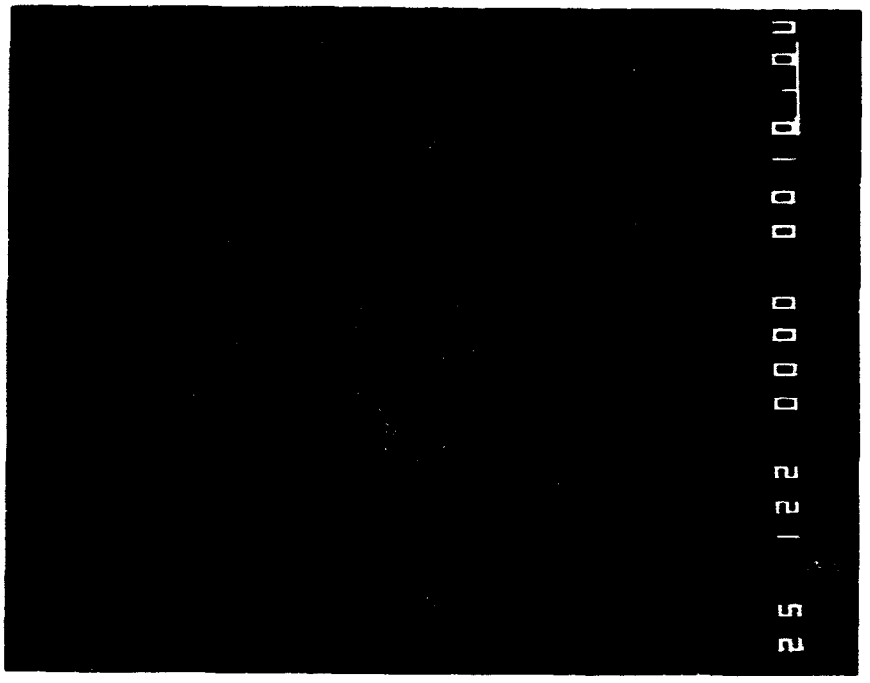

(d)

Figure 4. (Continued) X-ray dot map showing distributions of Mg (c) and Ca (d) in the Wesgo AL-600 material.

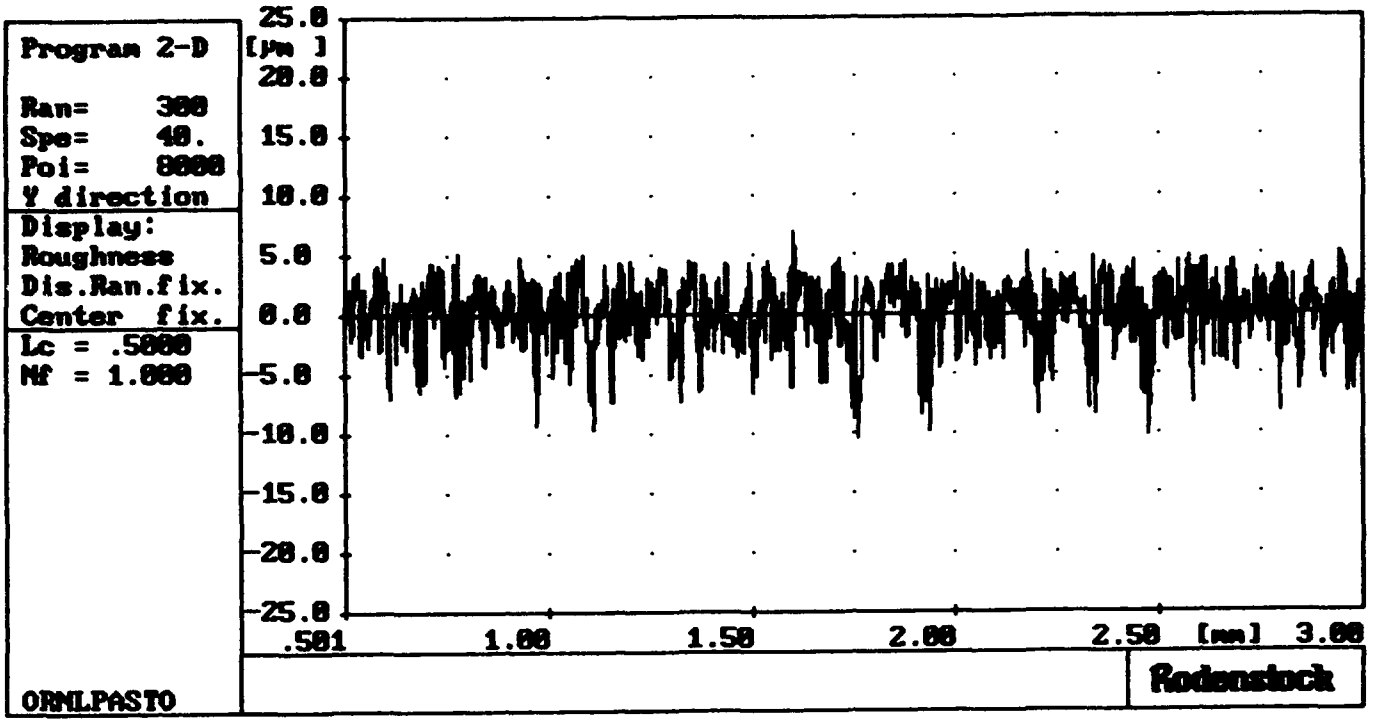

Figure 5. Display from the Rodenstock laser surface profilometer of the waviness across a longitudinally ground AL-600 alumina MOR bar prepared using Procedure 1.

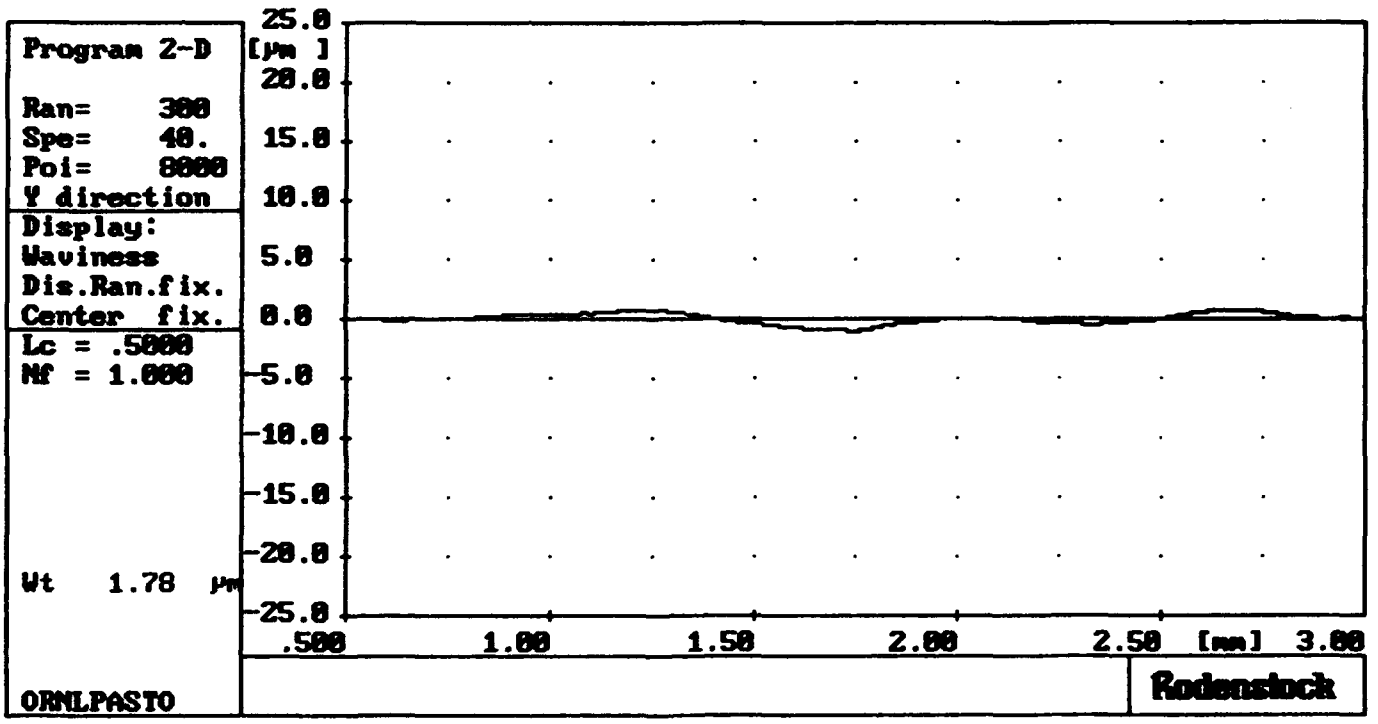

Figure 6. The roughness trace from the same MOR bar.

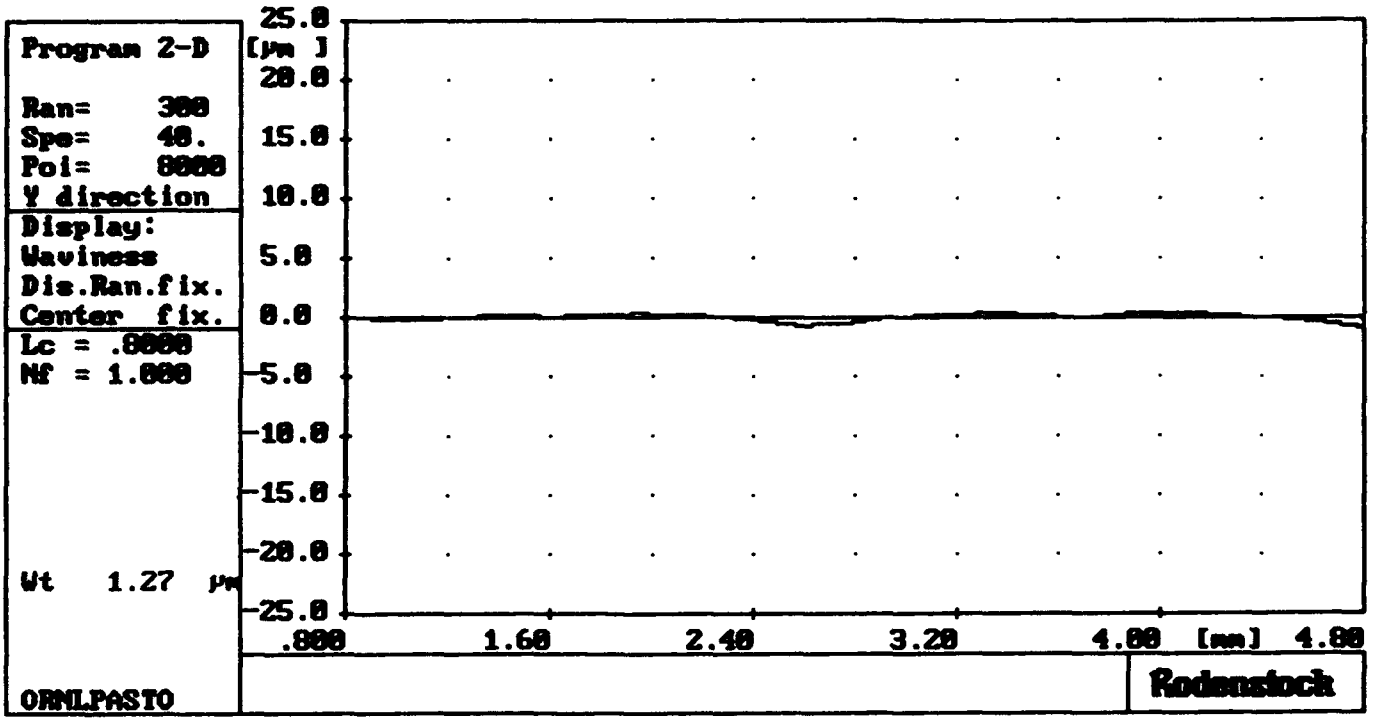

Figure 7. Display from the Rodenstock laser surface profilometer of the waviness across the end face of a compression cylinder made from AL-600 alumina, machined using Procedure 3.

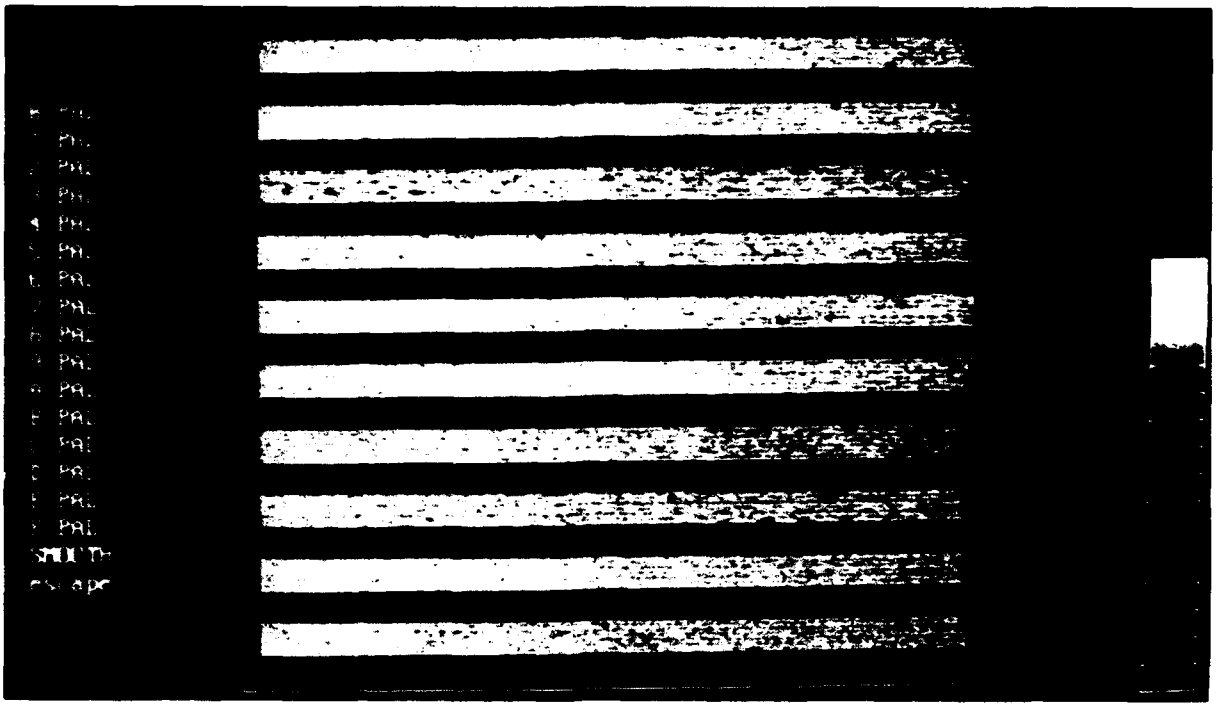

Figure 8. Photograph of ten AL-600 alumina MOR bars as viewed with a 50 MHz ultrasonic surface wave. Machined using Procedure #1.

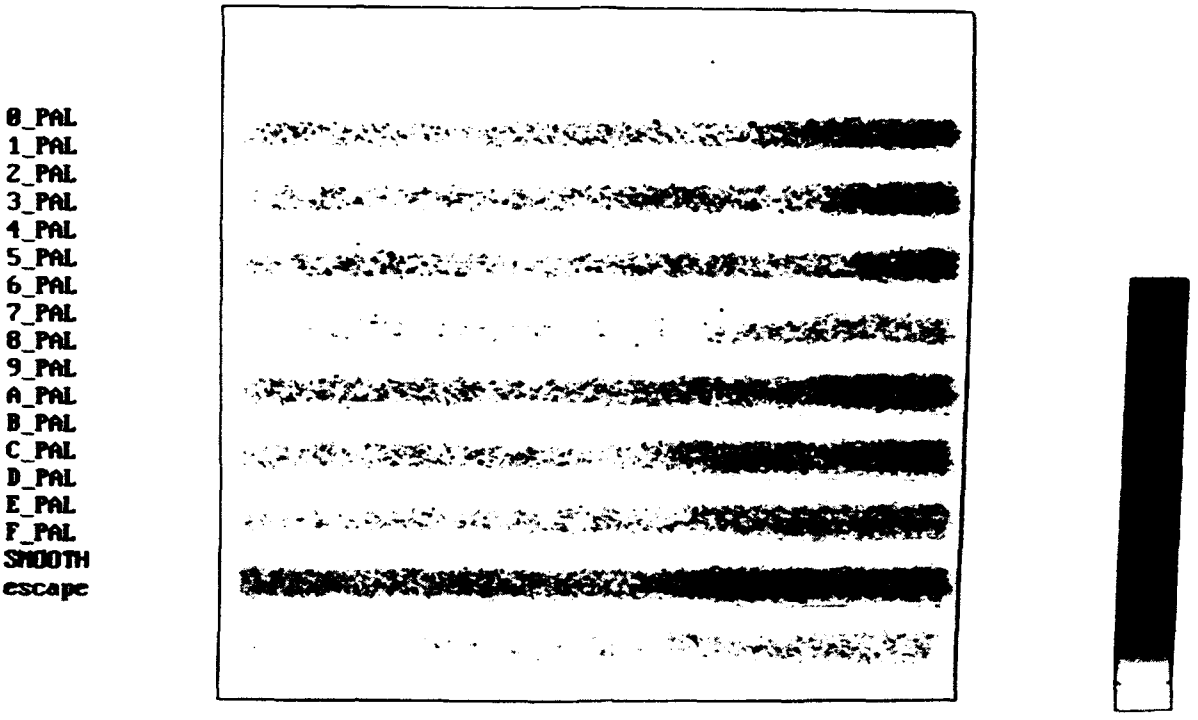

Figure 9. Photograph of the same alumina MOR bars shown in Figure 8 viewed with a 75 MHz ultrasonic transducer focussed at the bar midplane.

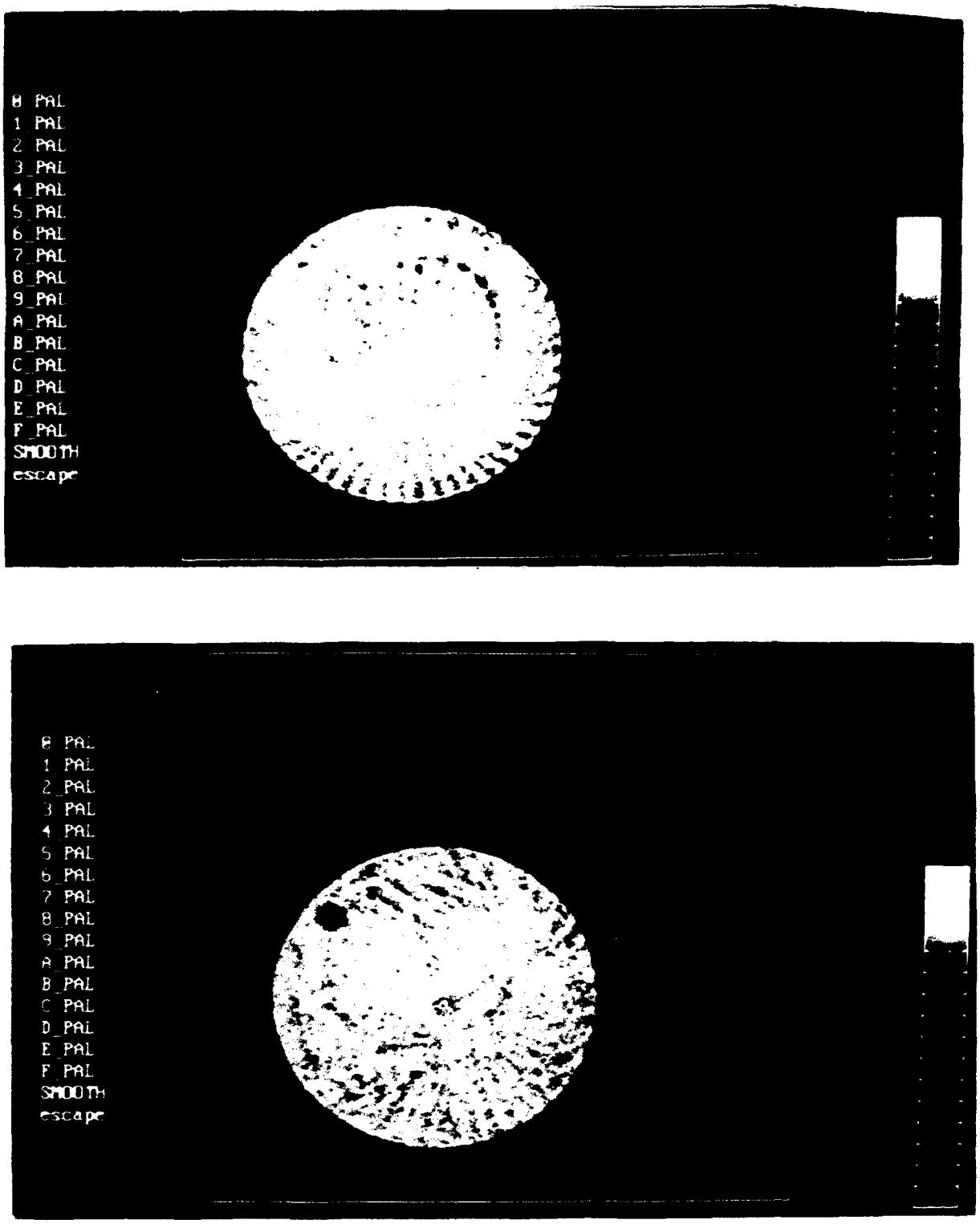

Figure 10. Photograph of a 13 mm (0.51 in.) diam alumina cylinder as viewed with a 50 MHz ultrasonic transducer. (a) top surface, (b) bottom surface. Faces machined by lathe turning the cylinder while sweeping the ends with a rotating wheel (Procedure 3).

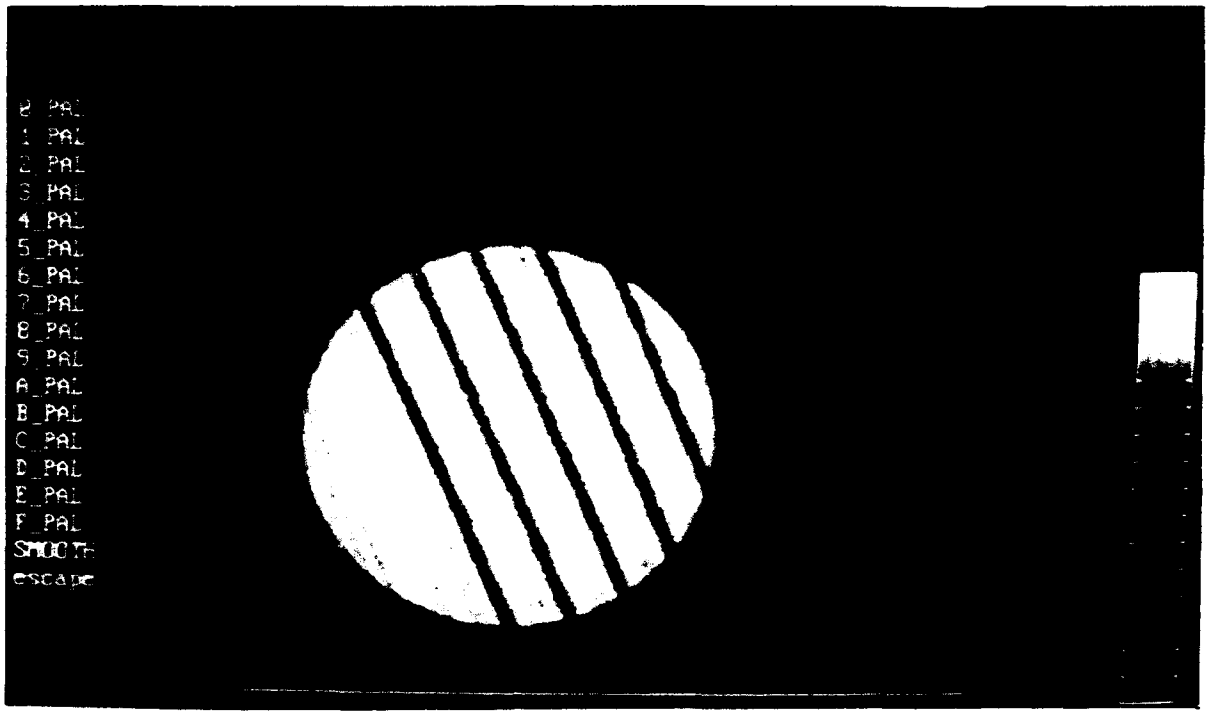

(a)

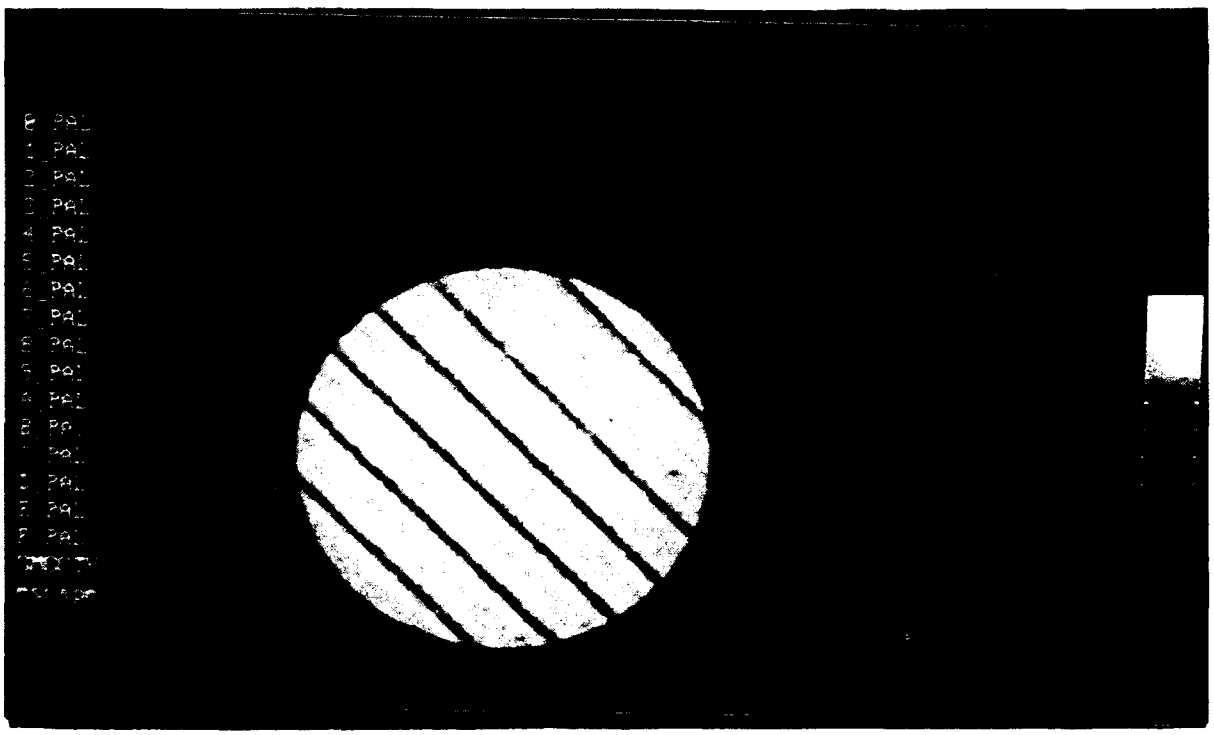

(b)

Figure 11. Photograph of a 13 mm (0.51 in.) diam Al-600 alumina cylinder as viewed with a 50 MHz ultrasonic transducer. (a) top surface, (b) bottom surface. Faces machined unidirectionally (Procedure 4).

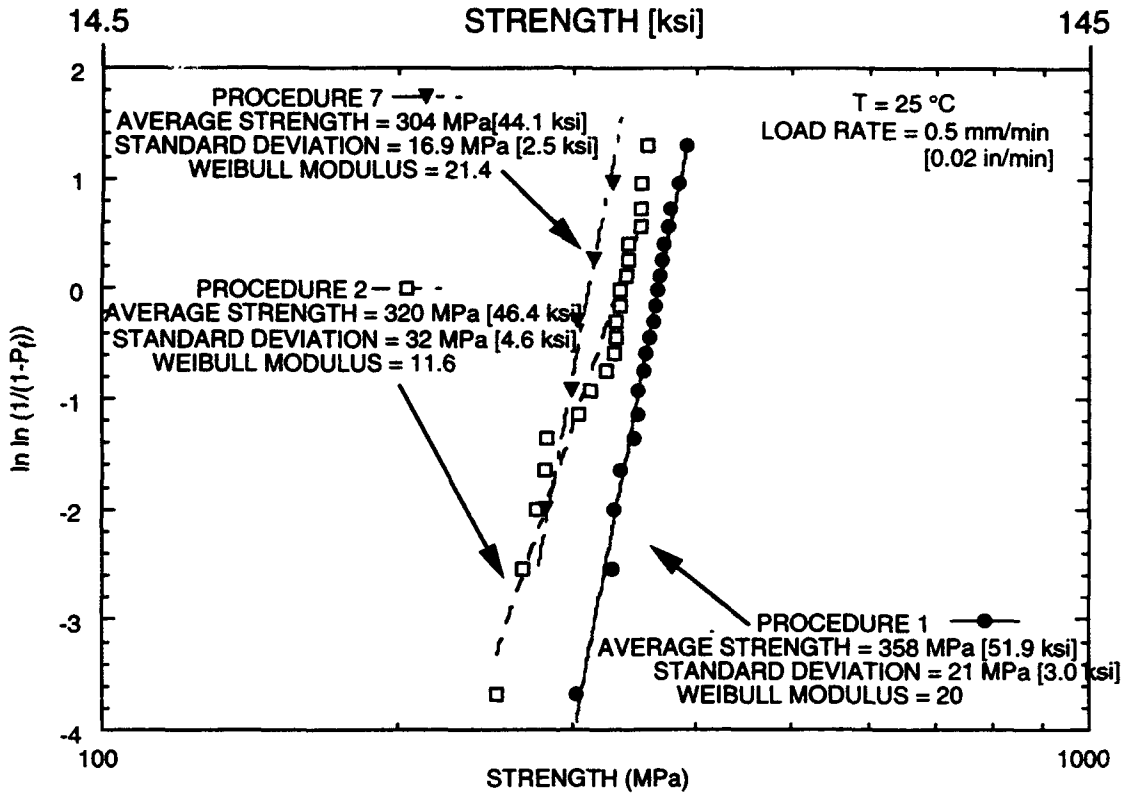

Figure 12. Weibull plots for MOR specimens of Wesgo AL-600 alumina machined using three different procedures.

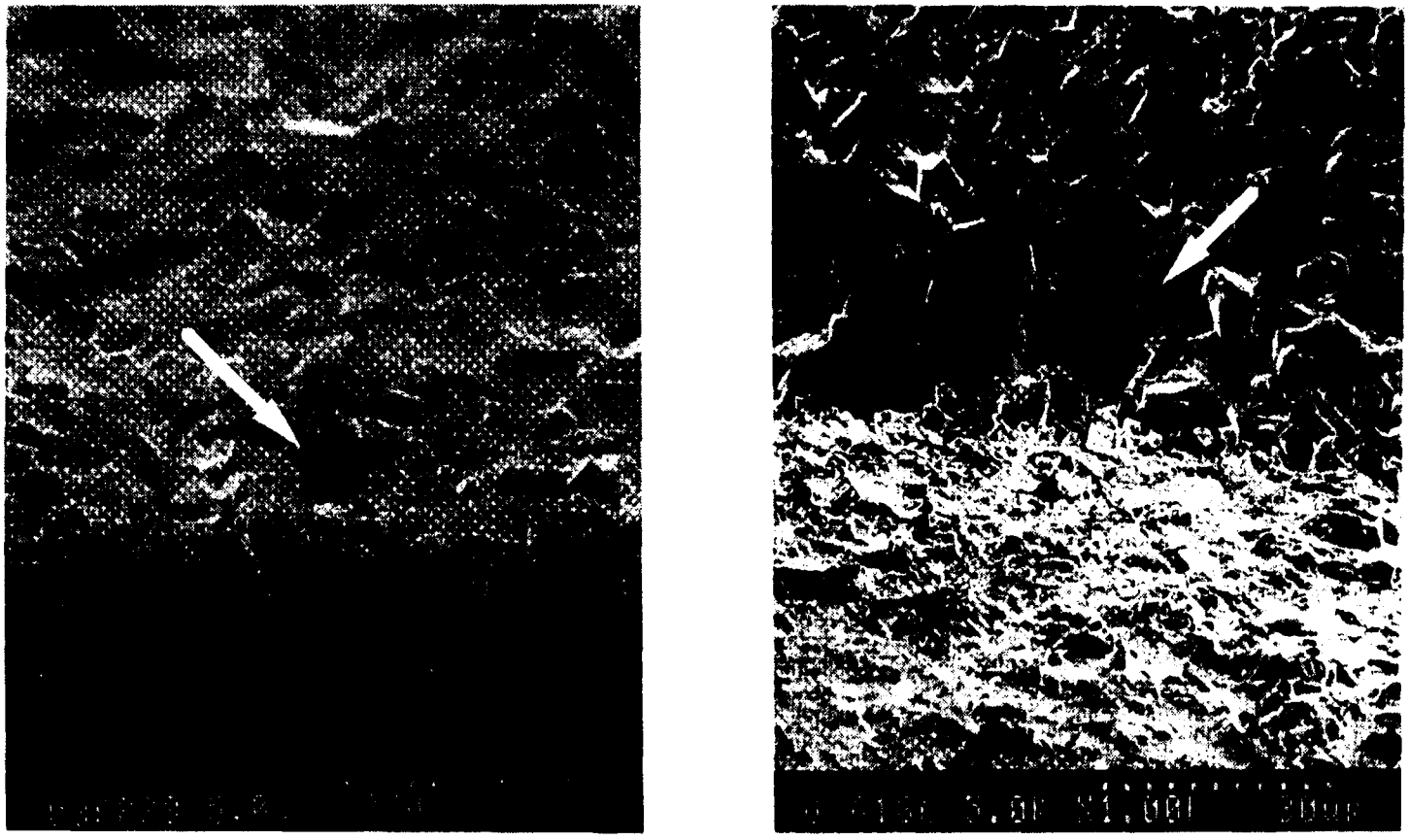

Figure 13. Scanning electron micrographs of fractured AL-600 alumina flexure specimens, showing typical critical defects (pores, at arrows). Specimen on left prepared by Grinding Procedure #1, specimen # 1B1-9. Specimen on right prepared by Grinding Procedure #2, specimen 2B2-1.

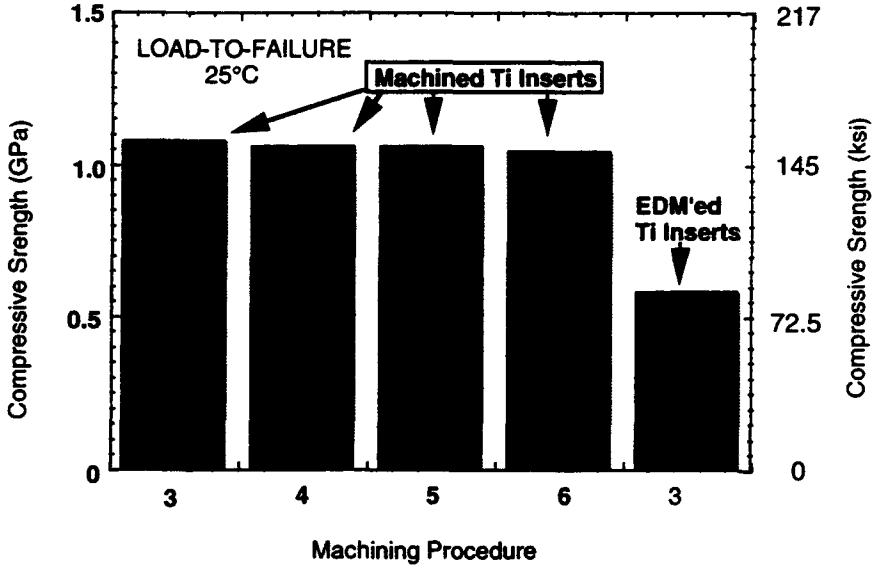

Figure 14. Effect of different grinding procedures on compressive strength of AL-600 alumina cylindrical specimens tested on titanium inserts.

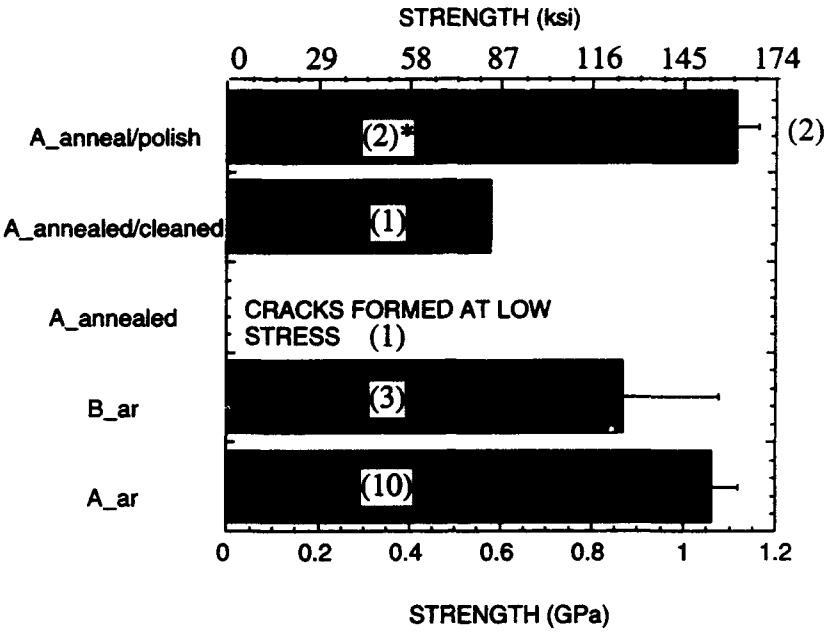

Figure 15. Compressive strength of AL-600 alumina cylindrical specimens as a function of Ti insert surface condition.
* Numbers of specimens tested in parentheses.

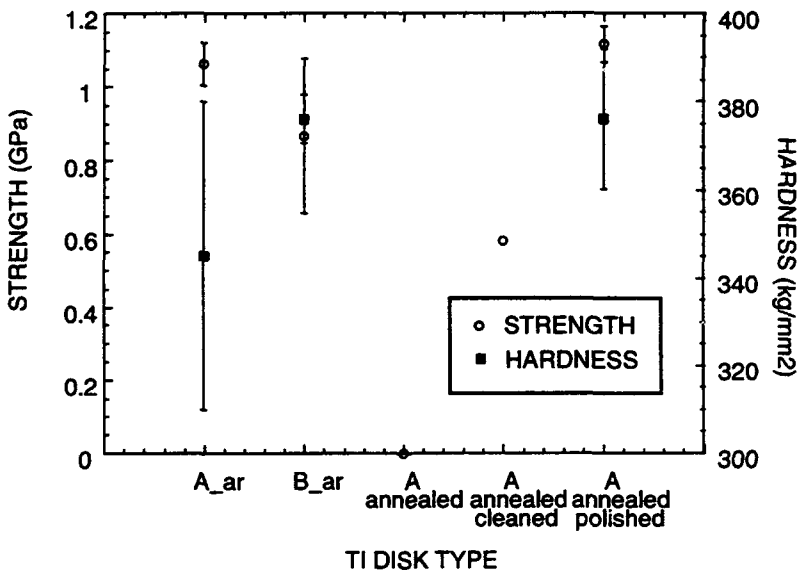

Figure 16. Compressive strength test results for the AL-600 alumina as a function of the surface condition of the Ti inserts, showing that the hardness of the Ti does not correlate to strength.

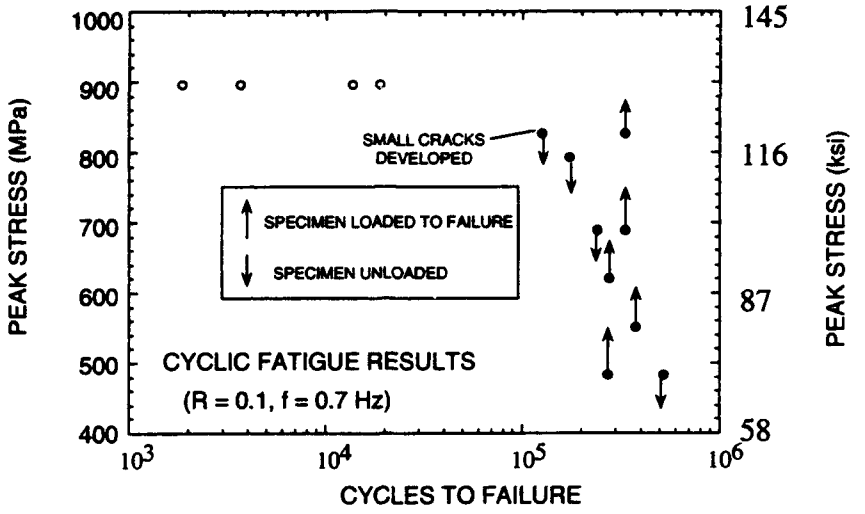

Figure 17. Compressive cyclic fatigue behavior of the AL-600 alumina cylindrical specimens. Open symbols represent failed specimens; closed symbols represent test which were terminated. For terminated specimens, upward facing arrows indicate specimens which were cycled to the prescribed number of cycles, then subsequently strength tested. Specimens with downward facing arrows were archived.

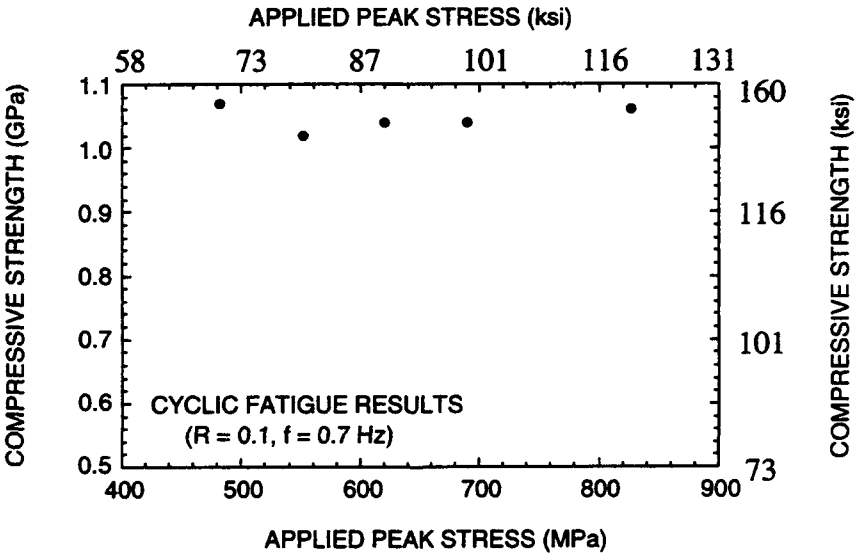

Figure 18. Compressive strength of cylindrical AL-600 alumina specimens previously cycled to different peak stresses shown above. The specimens were tested to failure on Ti inserts between steel anvils.

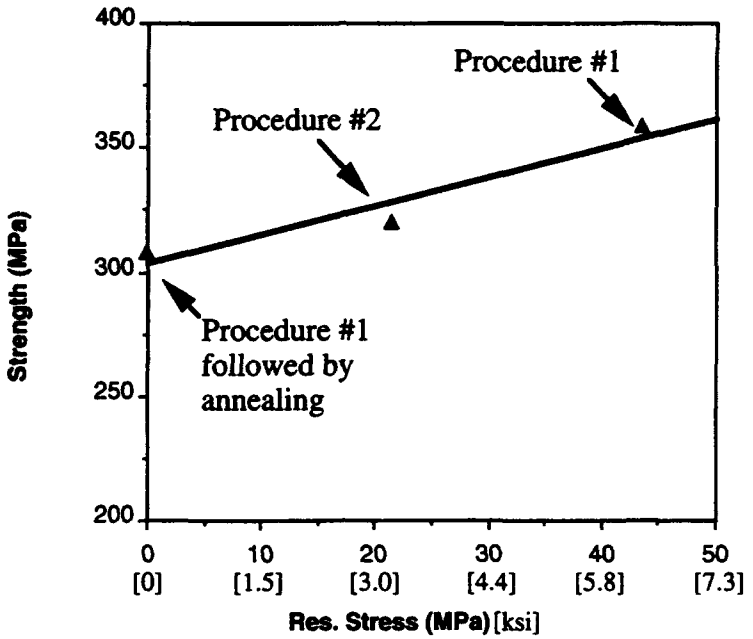

Figure 19. MOR strength of AL-600 alumina as a function of the compressive residual stress developed in the surface by machining. Data taken from Tables 5 and 6.

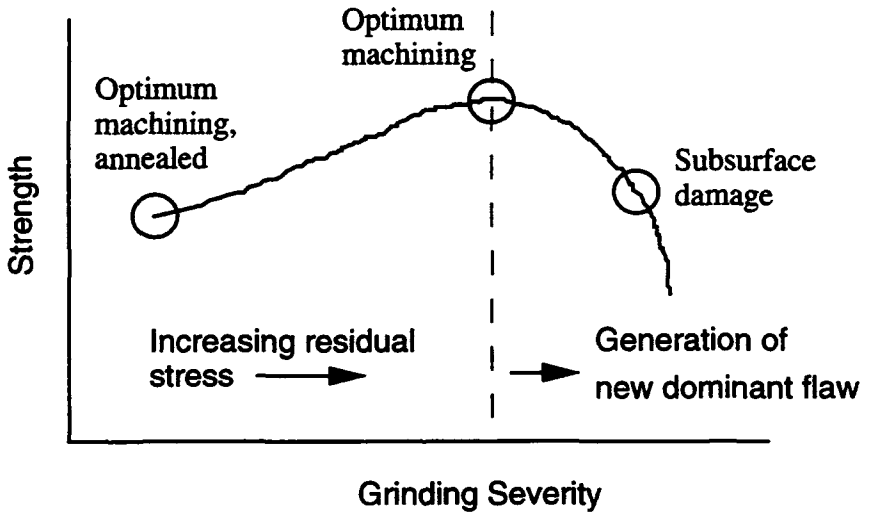

Figure 20. MOR strength of AL-600 alumina as a function of the "severity" of of the machining performed.

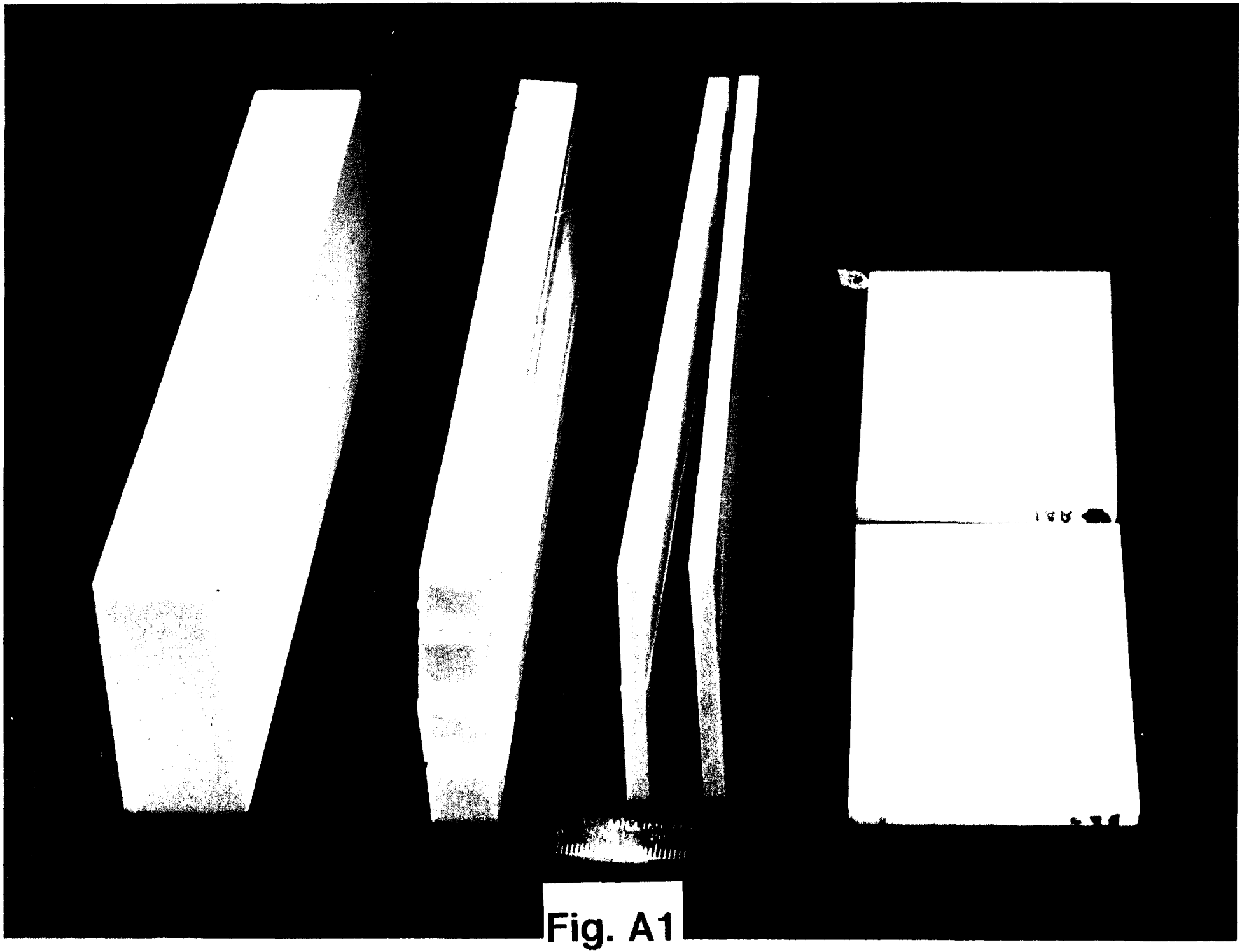

Fig. A1

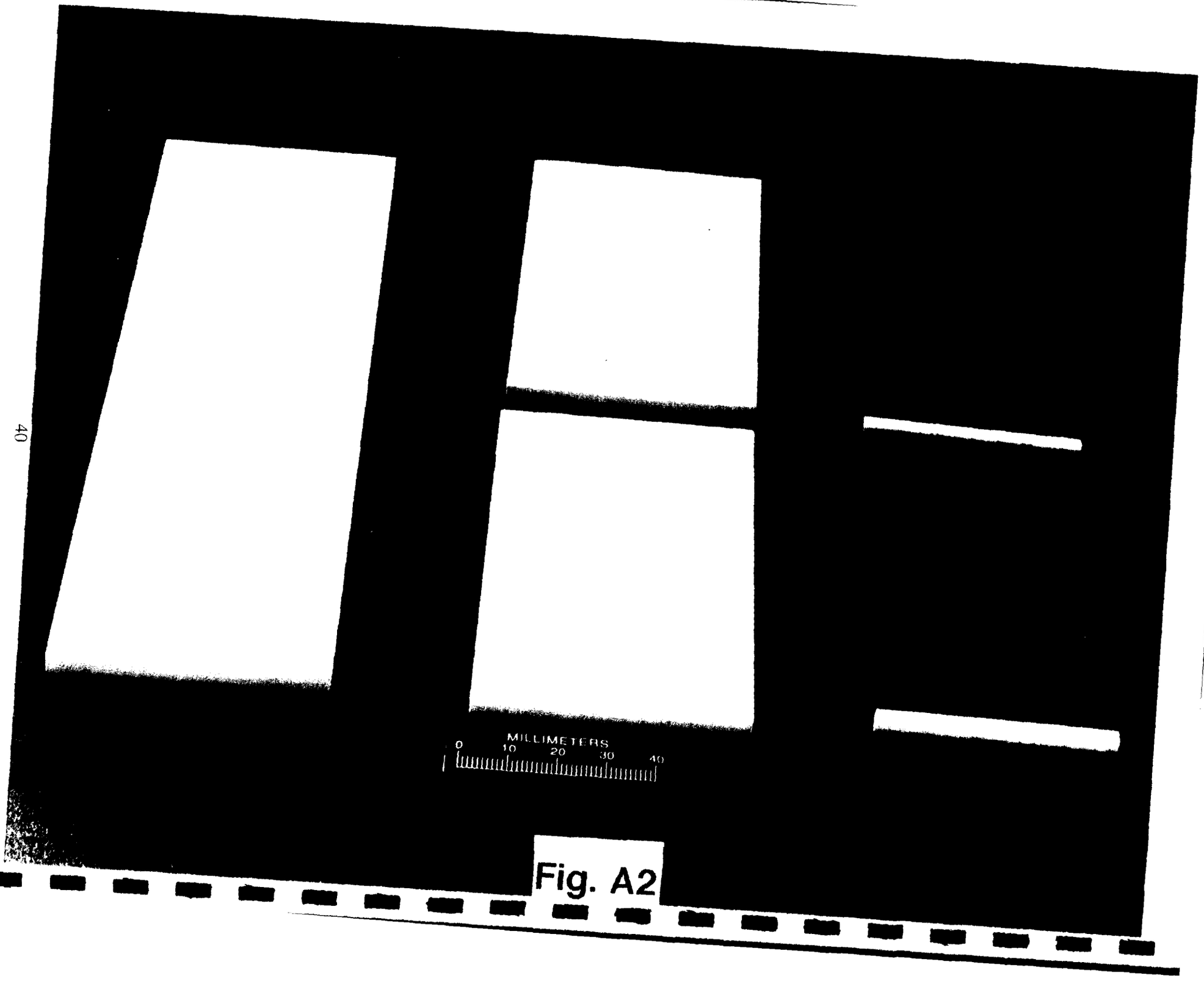

Fig. A2

Fig. A3

Fig. A4

Fig. A5

Fig. A6

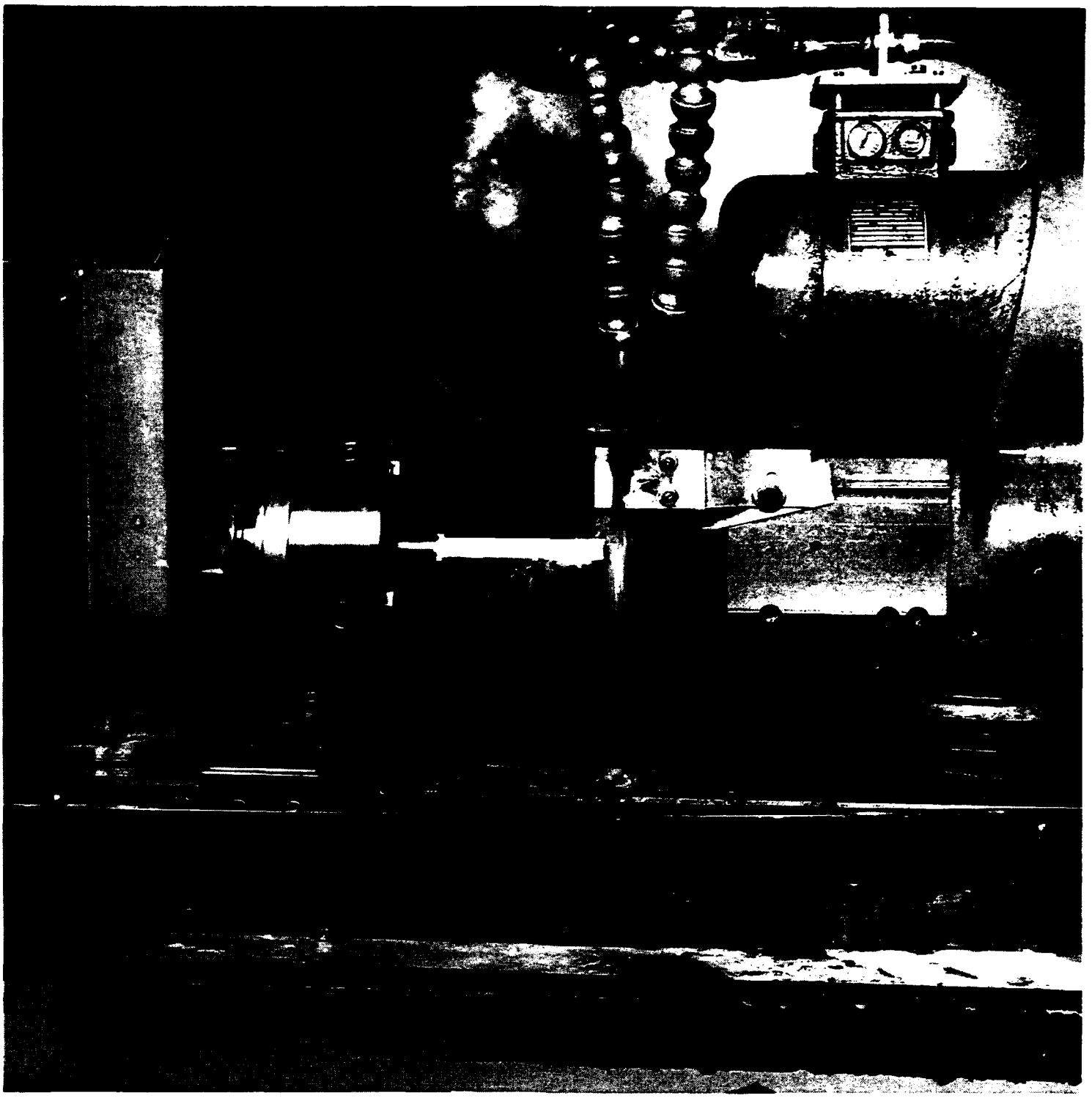

Fig. A7

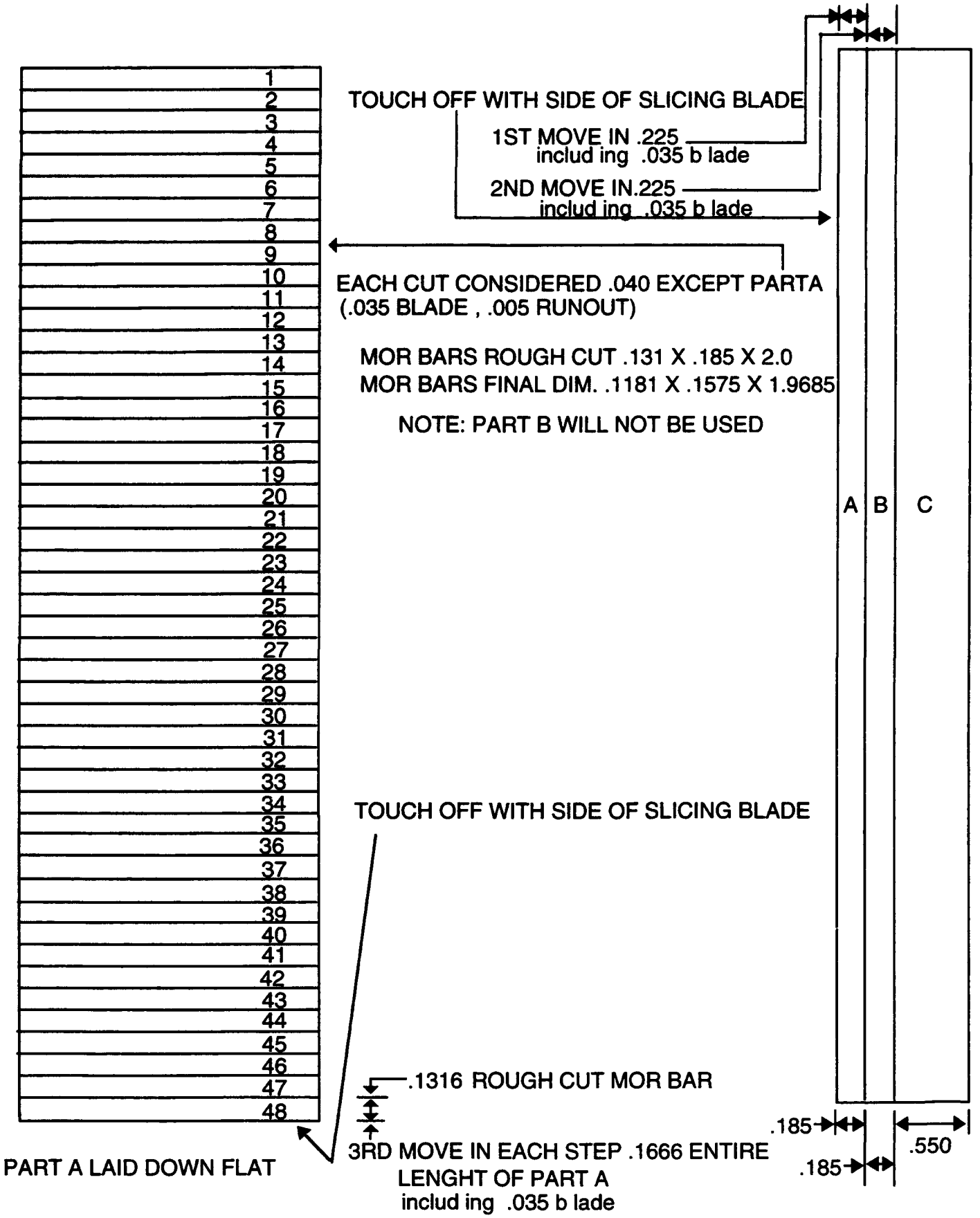

Figure A8. Sketch illustrating slicing paths for conversion of AL-600 alumina billets into MOR bars and cylindrical compression specimens.

APPENDIX A
MACHINING PROCEDURES

GENERAL PROCEDURE

The AL-600 alumina billets were received as $1 \times 4 \times 10$ in. billets which were sliced into halves as shown in Fig. A1 (left and center), with the halves subsequently being further machined into pieces suitable for slicing into either MOR bars or compression cylinders (center). The larger square cross-section pieces were utilized for cylinders, while the plates (right side, Fig. A1) were sliced into MOR bars as shown in Fig. A2. Slicing was performed on Harig 618 computer-numerically-controlled (CNC) surface grinders, shown in Fig. A3, using diamond cutting wheels as specified in the tables following.

MOR BARS AND RESIDUAL STRESS PLATES

The plates sliced from the billets were cemented onto the stage of the Harig grinders and ground flat and parallel using procedures detailed in the attached tables. (Fig. A4). These slabs were subsequently sliced (Fig. A5) into bars of the required dimensions on the same machines using diamond slicing wheels. Chamfers were ground into the edges of the bars at 45° angles with either a belt grinder and a fixture which placed the bars against the belt at the correct angle, or on the Harig grinders using the same wheels as were used for grinding the longitudinal faces of the bars.

CYLINDERS

Cylinders were prepared from the square section pieces of Fig. A1 by cylindrical grinding in a Jungner 4-axis grinder with diamond wheels, as shown in Fig. A6. The rods were then cut roughly to length in the same machine with a cutting wheel (Fig. A7). Final length dimension was obtained by either of two grinding methods: an omnidirectional finish was achieved by rotating the piece in the lathe chuck of the Jungner while a facing wheel counterrotated against the end (Fig. A8), or a unidirectional finish was achieved by holding the rod stationary in one of the Harig machines while a rotating grinding wheel was fed into the end of the cylinder.

Details of these procedures are listed in the following tables. Fig. A8 is a sketch of the billet with slicing paths overlain, to show the general scheme used for converting a billet into both MOR bars and cylindrical compression specimens.

CERAMIC MACHINING PROCEDURE #1

Specimen type MOR Bars **Job** Navy **Charge #** 3470-0412 **Material** Alumina AL-600

Specimen# 1B			**Manufacturer** Wesgo			
Operation	Slice Billet	Grind .1575 Dim	Slice Legth	Slice .130 Dim	Grind .118 dim.	Chamfer edges
Date Oper. Finished						
Machine	Harig NC	Harig CNC	Harig NC	Harig NC	Harig NC	Harig NC
Operator	Shelton	Shelton	O'Rourke	O'Rourke	O'Rourke	O'Rourke
Tool or Wheel type	8" X .035 Resin 100 100%	8" X .500 Resin 320 150%	8" X .035 Resin 100 100%	8" X .035 Resin 100 100%	6" x .250 Resin 120 100%	6" x .125 Resin 240 100%
Downfeed or Infeed	.0005	.0002	.003	.003	.0005	.005
Wheel speed	3400 Rpm	3600 Rpm	3400 Rpm	3400 Rpm	3400 Rpm	3400 Rpm
S.F.P.M.	5350	7550	7200	7200	5300	5300
Wheel or Tool Pos. Machining Direction	Wh. parallel longitudinal	Wh. parallel longitudinal	Wh. parallel longitudinal	Wh. parallel longitudinal	Wh. parallel longitudinal	Wh. parallel longitudinal
Wheel/Part Direction	Wh. CW	Wh. CW	Wh. CW	Wh. CW	Wh. CW	Wh. CW
Table/traverse speed	200in./min.	200in. /min.	100in./min.	100in./min.	75 in. /min.	100in./min.
Crossfeed	n/a	.050	n/a	n/a	.030	n/a
Workhead RPM	n/a	n/a	n/a	n/a	n/a	n/a
Coolant type	Buehler water sol.	Buehler water sol.	Buehler water sol.	Buehler water sol.	Buehler water sol.	Buehler water sol.
No. of Sparkouts	0	3	0	0	10	10
Oper.starting Dim.	2.25x1.0x8"	2.25x.185x8"	2.25x.1575x4	1.968x.1575x4	1.968x.157x.13	sharp corner
Oper. finishing Dim.	2.25x.185x8"	2.25x.1575x4	1.968x.1575x4.	1.968x.157x.13	1.968x.157x.118	45*x.007
Surf. Fin. RA / RQ	n/a	n/a	n/a	n/a	n/a	n/a
Inspection comments						

Comments

CERAMIC MACHINING PROCEDURE #1C

Specimen type MOR Bars **Job** Navy **Charge #** 3470-0412 **Material** Alumina AL-600

Specimen# 3B **Manufacturer** Wesgo

Operation	Slice Billet	Grind .1575 Dim	Slice Legth	Slice .130 Dim	Grind .118 dim.	Chamfer edges
Date Oper. Finished					4/13/93	
Machine	Harig NC	Harig CNC	Harig NC	Harig NC	Harig NC	
Operator	Shelton	Shelton	O'Rourke	O'Rourke	O'Rourke	O'Rourke
Tool or Wheel type	8" X .035 Resin 100 100%	6" X .500 Resin 120 100%	8" X .035 Resin 100 100%	8" X .035 Resin 100 100%	6" X .500 Resin 120 100%	
Downfeed or Infeed	.0005	.0002	.003	.003	.0002	
Wheel speed	3400 Rpm	3600 Rpm	3400 Rpm	3400 Rpm	3400 Rpm	
S.F.P.M.	5350	5300	7200	7200	5300	
Wheel or Tool Pos. Machining Direction	Wh. parallel longitudinal	Crossgrind	Wh. parallel longitudinal	Wh. parallel longitudinal	Crossgrind	
Wheel/Part Direction	Wh. CW	Wh. CW	Wh. CW	Wh. CW	Wh. CW	
Table/traverse speed	200in./min.	200in. /min.	100in./min.	100in./min.	75 in. /min.	
Crossfeed	n/a	.050	n/a	n/a	.050	n/a
Workhead RPM	n/a	n/a	n/a	n/a	n/a	n/a
Coolant type	Buehler water sol.	Buehler water sol.	Buehler water sol.	Buehler water sol.	Buehler water sol.	
No. of Sparkouts	0	3	0	0	10	
Oper.starting Dim.	2.25x1.0x8"	2.25x.185x8"	2.25x.1575x4	1.968x.1575x4	1.968x.157x.13	sharp corner
Oper. finishing Dim.	2.25x.185x8"	2.25x.1575x4	1.968x.1575x4.	1.968x.157x.13	1.968x.157x.118	45*x.007
Surf. Fin. RA / RQ	n/a	n/a	n/a	n/a	n/a	n/a
Inspection comments						

Comments

CERAMIC MACHINING PROCEDURE #2

Specimen type 30x30 mm **Job** Navy **Charge #** 3470-0412 **Material** Alumina AL-600

Specimen#	Billet 7A2		**Manufacturer** WESGO			
Operation	Slice Billet	Surf Grind	Grind 4 edges			
Date Oper. Finished	3/17/93	3/18/93	3/22/93			
Machine	Harig CNC	Harig CNC	Harig CNC			
Operator	Shelton	Shelton	Shelton			
Tool or Wheel type	6"x .035 Resin 100 100%	8" x .5 Resin 320 150%	8" x .5 Resin 320 150%			
Downfeed or Infeed	.0005	.0005	.0005			
Wheel speed	3400 rpm	3600 rpm	3600 rpm			
S.F.P.M.	5350	7550	7550			
Wheel or Tool Pos. Machining Direction	Wh.Parallel longitudinal	Wh.Parallel longitudinal	Wh.Parallel longitudinal			
Wheel/Part Direction	wh. CW	wh. CW	wh. CW			
Table/traverse speed	200in / min.	200in / min.	200in / min.			
Crossfeed	n/a	.050	.030			
Workhead RPM	n/a	n/a	n/a			
Coolant type	Buehler Water Sol.	Buehler Water Sol.	Buehler Water Sol.			
No. of Sparkouts	n/a	3	0			
Oper.starting Dim.	2.25x4.0x.181	1.25x1.25x.181	1.25x1.25x.158			
Oper. finishing Dim.	1.25x1.25x.181	1.25x1.25x.158	1.181x1.181x.158			
Surf. Fin. RA / RQ	n/a	n/a	n/a			
Inspection comments						

Comments In all machining operations the Buehler Water Soluble coolant has been filtered with a Darenth Filteration system using a 5-15 micron filteration paper.

All edges ground in the longitudinal direction. Delivered to Tom Watkins 3/22/93
1 Specimen

CERAMIC MACHINING PROCEDURE #2

Specimen type MOR Bars **Job** Navy **Charge #** 3470-0412 **Material** Alumina AL-600

Specimen# 2B			**Manufacturer** Wesgo			
Operation	Slice Billet	Grind .1575 Dim	Slice Legth	Slice .130 Dim	Grind .118 dim.	Chamfer edges
Date Oper. Finished						3-30-93
Machine	Harig NC	Harig CNC	Harig NC	Harig NC	Harig NC	Harig NC
Operator	Shelton	Shelton	O'Rourke	O'Rourke	O'Rourke	O'Rourke
Tool or Wheel type	8" X .035 Resin 100 100%	8" X .500 Resin 320 150%	8" X .035 Resin 100 100%	8" X .035 Resin 100 100%	8" x .500 Resin 320 150%	8" x .500 Resin 320 150%
Downfeed or Infeed	.0005	.0002	.003	.003	.0005	.005
Wheel speed	3400 Rpm	3600 Rpm	3400 Rpm	3400 Rpm	3400 Rpm	3400 Rpm
S.F.P.M.	5350	7550	7200	7200	7200	7200
Wheel or Tool Pos. Machining Direction	Wh.Parallel longitudinal	Wh.Parallel longitudinal	Wh. perp. traverse	Wh.Parallel longitudinal	Wh.Parallel longitudinal	Wh.Parallell ongitudinal
Wheel/Part Direction	Wh. CW	Wh. CW	Wh. CW	Wh. CW	Wh. CW	Wh. CW
Table/traverse speed	200in./min.	200in. /min.	100in./min.	100in./min.	100in./min.	100in./min.
Crossfeed	n/a	.050	n/a	n/a	.030	n/a
Workhead RPM	n/a	n/a	n/a	n/a	n/a	n/a
Coolant type	Buehler water sol.	Buehler water sol.	Buehler water sol.	Buehler water sol.	Buehler water sol.	Buehler water sol.
No. of Sparkouts	0	3	0	0	10	10
Oper.starting Dim.	2.25x1.0x8"	2.25x.185x8"	2.25x.1575x4	1.968x.1575x4	1.968x.157x.13	sharp corner
Oper. finishing Dim.	2.25x.185x8"	2.25x.1575x4	1.968x.1575x4.	1.968x.157x.13	1.968x.157x.118	45*x.007
Surf. Fin. RA / RQ	n/a	n/a	n/a	n/a	n/a	n/a
Inspection comments						#24 chipped

Comments

CERAMIC MACHINING PROCEDURE #1,2A

Specimen type 30x30mm **Job** Navy **Charge #** 3470-0412 **Material** Alumina AL600

Specimen#	Billet Slice 1A1		**Manufacturer** WESGO			
Operation	Slice Billet	GrindEdges	RoughGrind	SemiGrind		
Date Oper. Finished	3/26/93	3/29/93	3/30/93	3/30/93		
Machine	Harig CNC	Harig CNC	Harig CNC	Harig CNC		
Operator	Shelton	Shelton	Shelton	Shelton		
Tool or Wheel type	6"x.035 Resin 100 100%	8"x.500 Resin 320 150%	6"x.500 Resin 120 100%	8"x.500 Resin 320 150%		
Downfeed or Infeed	.0005	.0002	.002	.0005		
Wheel speed	3400	3600	6050	4535		
S.F.P.M.	5350	7550	9500	9500		
Wheel or Tool Pos. Machining Direction	Wh.Parallel longitudinal	Wh.Parallel longitudinal	Wh.Parallel longitudinal	Wh.Parallel longitudinal		
Wheel/Part Direction	Wh. CW	Wh. CW	Wh. CW	Wh. CW		
Table/traverse speed	200 in/min	200 in/min	360 in/min	200 in/min		
Crossfeed	0	.050	.050	.080		
Workhead RPM	n/a	n/a	n/a	n/a		
Coolant type	Buehler Water Sol.	Buehler Water Sol.	Buehler Water Sol.	Buehler Water Sol.		
No. of Sparkouts	0	3	5	10		
Oper.starting Dim.	2.25x4.0x.197	1.2x1.2x.197	.181 thick	.171 thick		
Oper. finishing Dim.	1.2x1.2x.197	1.181x1.181	.171 thick	.161 thick		
Surf. Fin. RA / RQ	n/a	n/a	n/a	n/a		
Inspection comments						

Comments In all machining operations the Buehler Water Soluble coolant has been filtered with a Darenth Filteration system using a 5-15 micron filteration paper.

Delivered to Tom Watkins 3/26/93

CERAMIC MACHINING PROCEDURE #2

Specimen type MOR Bars **Job** Navy **Charge #** 3470-0412 **Material** Alumina AL-600

Specimen# 4A **Manufacturer** Wesgo

Operation	Slice Billet	Grind .1575 Dim	Slice Legth	Slice .130 Dim	Grind .118 dim.	Chamfer edges
Date Oper. Finished				30 MAR 93	4/19/93	
Machine	Harig NC	Harig CNC	Harig NC	Harig NC	Harig NC	
Operator	Shelton	Shelton	O'Rourke	O'Rourke	O'Rourke	O'Rourke
Tool or Wheel type	8" X .035 Resin 100 100%	8" X .500 Resin 320 150%	8" X .035 Resin 100 100%	8" X .035 Resin 100 100%	8" x .500 Resin 320 150%	
Downfeed or Infeed	.0005	.0002	.003	.003	.0005	
Wheel speed	3400 Rpm	3600 Rpm	3400 Rpm	3400 Rpm	3400 Rpm	
S.F.P.M.	5350	7550	7200	7200	7200	
Wheel or Tool Pos. Machining Direction	Wh.Parallel longitudinal	Wh.Parallel longitudinal	Wh. perp. traverse	Wh.Parallel longitudinal	Wh.Parallel longitudinal	
Wheel/Part Direction	Wh. CW	Wh. CW	Wh. CW	Wh. CW	Wh. CW	
Table/traverse speed	200in./min.	200in. /min.	100in./min.	100in./min.	100in./min.	
Crossfeed	n/a	.050	n/a	n/a	.030	n/a
Workhead RPM	n/a	n/a	n/a	n/a	n/a	n/a
Coolant type	Buehler water sol.	Buehler water sol.	Buehler water sol.	Buehler water sol.	Buehler water sol.	
No. of Sparkouts	0	3	0	0	10	
Oper.starting Dim.	2.25x1.0x8"	2.25x.185x8"	2.25x.1575x4	1.968x.1575x4	1.968x.157x.13	sharp corner
Oper. finishing Dim.	2.25x.185x8"	2.25x.1575x4	1.968x.1575x4.	1.968x.157x.13	1.968x.157x.118	45*x.007
Surf. Fin. RA / RQ	n/a	n/a	n/a	n/a	n/a	n/a
Inspection comments						

Comments

CERAMIC MACHINING PROCEDURE #2

Specimen type MOR Bars **Job** Navy **Charge #** 3470-0412 **Material** Alumina AL-600

Specimen# 5A			**Manufacturer** Wesgo			
Operation	Slice Billet	Grind .1575 Dim	Slice Legth	Slice .130 Dim	Grind .118 dim.	Chamfer edges
Date Oper. Finished				30 MAR 93		
Machine	Harig NC	Harig CNC	Harig NC	Harig NC	Harig NC	Harig NC
Operator	Shelton	Shelton	O'Rourke	O'Rourke	O'Rourke	O'Rourke
Tool or Wheel type	8" X .035 Resin 100 100%	8" X .500 Resin 320 150%	8" X .035 Resin 100 100%	8" X .035 Resin 100 100%	8" x .500 Resin 320 150%	8" x .500 Resin 320 150%
Downfeed or Infeed	.0005	.0002	.003	.003	.0005	.005
Wheel speed	3400 Rpm	3600 Rpm	3400 Rpm	3400 Rpm	3400 Rpm	3400 Rpm
S.F.P.M.	5350	7550	7200	7200	7200	7200
Wheel or Tool Pos. Machining Direction	Wh.Parallel longitudinal	Wh.Parallel longitudinal	Wh. perp. traverse	Wh.Parallel longitudinal	Wh.Parallel longitudinal	Wh.Parallell ongitudinal
Wheel/Part Direction	Wh. CW	Wh. CW	Wh. CW	Wh. CW	Wh. CW	Wh. CW
Table/traverse speed	200in./min.	200in. /min.	100in./min.	100in./min.	100in./min.	100in./min.
Crossfeed	n/a	.050	n/a	n/a	.030	n/a
Workhead RPM	n/a	n/a	n/a	n/a	n/a	n/a
Coolant type	Buehler water sol.	Buehler water sol.	Buehler water sol.	Buehler water sol.	Buehler water sol.	Buehler water sol.
No. of Sparkouts	0	3	0	0	10	10
Oper.starting Dim.	2.25x1.0x8"	2.25x.185x8"	2.25x.1575x4	1.968x.1575x4	1.968x.157x.13	sharp corner
Oper. finishing Dim.	2.25x.185x8"	2.25x.1575x4	1.968x.1575x4.	1.968x.157x.13	1.968x.157x.118	45*x.007
Surf. Fin. RA / RQ	n/a	n/a	n/a	n/a	n/a	n/a
Inspection comments						

Comments

CERAMIC MACHINING PROCEDURE #2

Specimen type MOR Bars **Job** Navy **Charge #** 3470-0412 **Material** Alumina AL-600

Specimen# 4B **Manufacturer** Wesgo

Operation	Slice Billet	Grind .1575 Dim	Slice Legth	Slice .130 Dim	Grind .118 dim.	Chamfer edges
Date Oper. Finished					4/13/93	
Machine	Harig NC	Harig CNC	Harig NC	Harig NC	Harig NC	
Operator	Shelton	Shelton	O'Rourke	O'Rourke	O'Rourke	O'Rourke
Tool or Wheel type	8" X .035 Resin 100 100%	8" X .500 Resin 320 150%	8" X .035 Resin 100 100%	8" X .035 Resin 100 100%	8" X .500 Resin 320 150%	
Downfeed or Infeed	.0005	.0005	.003	.003	.0005	
Wheel speed	3400 Rpm	3600 Rpm	3400 Rpm	3400 Rpm	3400 Rpm	
S.F.P.M.	5350	7550	7200	7200	5300	
Wheel or Tool Pos. Machining Direction	Wh. parallel longitudinal	Crossgrind	Wh. parallel longitudinal	Wh. parallel longitudinal	Crossgrind	
Wheel/Part Direction	Wh. CW	Wh. CW	Wh. CW	Wh. CW	Wh. CW	
Table/traverse speed	200in./min.	200in. /min.	100in./min.	100in./min.	75 in. /min.	
Crossfeed	n/a	.050	n/a	n/a	.050	n/a
Workhead RPM	n/a	n/a	n/a	n/a	n/a	n/a
Coolant type	Buehler water sol.	Buehler water sol.	Buehler water sol.	Buehler water sol.	Buehler water sol.	
No. of Sparkouts	0	3	0	0	10	
Oper.starting Dim.	2.25x1.0x8"	2.25x.185x8"	2.25x.1575x4	1.968x.1575x4	1.968x.157x.13	sharp corner
Oper. finishing Dim.	2.25x.185x8"	2.25x.1575x4	1.968x.1575x4.	1.968x.157x.13	1.968x.157x.118	45*x.007
Surf. Fin. RA / RQ	n/a	n/a	n/a	n/a	n/a	n/a
Inspection comments						

Comments

CERAMIC MACHINING PROCEDURE #2

Specimen type MOR BAR **Job** Navy **Charge #** 3470-0412 **Material** Ad-94

Specimen#	longitudinal of tube		**Manufacturer** Coors			
Operation	Slice Billet	Grind .1575 Dim	Slice Legth	Slice .130 Dim	Grind .118 dim.	Chamfer edges
Date Oper. Finished						
Machine	Harig NC	Harig CNC	Harig NC	Harig NC	Harig NC	Belt sander
Operator	O'Rourke	O'Rourke	O'Rourke	O'Rourke	O'Rourke	O'Rourke
Tool or Wheel type	8" X .035 Resin 100 100%	8" X .500 Resin 320 150%	6" X .035 Resin 100 100%	6" X .035 Resin 100 100%	6" x .250 Resin 320 100%	1x42 belt 220 Grit
Downfeed or Infeed	.001	.0005	.001	.001	.0005	n/a
Wheel speed	3400 Rpm	3400 Rpm	3400 Rpm	3400 Rpm	3400 Rpm	1725
S.F.P.M.	5300	5300	5300	5300	5300	1800
Wheel or Tool Pos. Machining Direction	Wh. parallel longitudinal	Wh. parallel longitudinal	Wh. parallel longitudinal	Wh. parallel longitudinal	Wh. parallel longitudinal	Wh. parallel longitudinal
Wheel/Part Direction	Wh. CW	Wh. CW	Wh. CW	Wh. CW	Wh. CW	Wh. CW
Table/traverse speed	75in./min.	100in. /min.	100in./min.	100in./min.	100in/min	n/a
Crossfeed	n/a	.030	n/a	n/a	.030	n/a
Workhead RPM	n/a	n/a	n/a	n/a	n/a	n/a
Coolant type	Buehler water sol.	Buehler water sol.	Buehler water sol.	Buehler water sol.	Buehler water sol.	n/a
No. of Sparkouts	0	10	0	0	10	n/a
Oper.starting Dim.	2.4x4.3x.640	2.4x4.3x.185	2.4x4.3x.157	1.968x.1575x4.	1.968x.157x.13	sharp corner
Oper. finishing Dim.	2.4x4.3x.185	2.4x4.3x.157	1.968x.1575x4.3	1.968x.157x.13	1.968x.157x.118	45*x.007
Surf. Fin. RA / RQ	n/a	n/a	n/a	n/a	n/a	n/a
Inspection comments				Gang sliced 5 at a time		

Comments

longitudinal X longitudinal

CERAMIC MACHINING PROCEDURE #2

Specimen type MOR BAR **Job** Navy **Charge #** 3470-0412 **Material** AD-94

Specimen#	perpindicular of tube		**Manufacturer** Coors			
Operation	Slice Billet	Grind .1575 Dim	Slice Legth	Slice .130 Dim	Grind .118 dim.	Chamfer edges
Date Oper. Finished						
Machine	Harig NC	Harig CNC	Harig NC	Harig NC	Harig NC	Belt sander
Operator	O'Rourke	O'Rourke	O'Rourke	O'Rourke	O'Rourke	O'Rourke
Tool or Wheel type	8" X .035 Resin 100 100%	8" X .500 Resin 320 150%	6" X .035 Resin 100 100%	6" X .035 Resin 100 100%	6" x .250 Resin 320 100%	1x42 belt 220 Grit
Downfeed or Infeed	.001	.0005	.001	.001	.0005	n/a
Wheel speed	3400 Rpm	3400 Rpm	3400 Rpm	3400 Rpm	3400 Rpm	1725
S.F.P.M.	5300	5300	5300	5300	5300	1800
Wheel or Tool Pos. Machining Direction	Wh. parallel longitudinal	Wh. parallel longitudinal	Wh. parallel longitudinal	Wh. parallel longitudinal	Wh. parallel longitudinal	Wh. parallel longitudinal
Wheel/Part Direction	Wh. CW	Wh. CW	Wh. CW	Wh. CW	Wh. CW	Wh. CW
Table/traverse speed	75in./min.	100in. /min.	100in./min.	100in./min.	100in/min	n/a
Crossfeed	n/a	.030	n/a	n/a	.030	n/a
Workhead RPM	n/a	n/a	n/a	n/a	n/a	n/a
Coolant type	Buehler water sol.	Buehler water sol.	Buehler water sol.	Buehler water sol.	Buehler water sol.	n/a
No. of Sparkouts	0	10	0	0	10	n/a
Oper.starting Dim.	2.4x4.3x.640	2.4x4.3x.185	2.4x4.3x.157	1.968x.1575x4.	1.968x.157x.13	sharp corner
Oper. finishing Dim.	2.4x4.3x.185	2.4x4.3x.157	1.968x.1575x4.3	1.968x.157x.13	1.968x.157x.118	45*x.007
Surf. Fin. RA / RQ	n/a	n/a	n/a	n/a	n/a	n/a
Inspection comments				Gang sliced 5 at a time		

Comments sliced out of raw material from tube perpindicular to the original longitudinal ground specimens then ground longitudinal to the way they were sliced out

CERAMIC MACHINING PROCEDURE #3

Specimen type Compr. Spec. **Job** Navy **Charge #** 3470-0412 **Material** Alumina AL-600

Specimen#	REFER BOTTOM	**Manufacturer** Wesgo				
Operation	Slice Billet	Rough OD	Finish OD	Rough lenght	Finish Lenght	chamfer ends
Date Oper. Finished						
Machine	Harig NC	Jungner	Jungner	Jungner	Jungner	Jungner
Operator	Jenkins	Jenkins	Jenkins	Jenkins	Jenkins	Jenkins
Tool or Wheel type	8"x .035 Resin 100 100%	8" x .5 Resin 320 150%	8" x .5 Resin 320 150%	8"x .035 Resin 100 100%	8" x .5 Process E 200/230grit	8" x .5 Resin 320 150%
Downfeed or Infeed	.0005	.0002	.0002	.001	.001	.0002
Wheel speed	3400 rpm	3400 rpm	3400 rpm	3400 rpm	3400 rpm	3400 rpm
S.F.P.M.	7125	7125	7125	7125	7125	7125
Wheel or Tool Pos. Machining Direction	Wh. parallel longitudinal	Wh. perp. longitudinal	Wh. perp. longitudinal	Wh. perp. longitudinal	Wh. perp. traverse	part on 45* traverse
Wheel/Part Direction	Wh. CW	opposite	opposite	opposite	opposite	opposite
Table/traverse speed	50 in / min.	40 in / min.	20 in / min.	100 in / min	50 in / min.	20 in / min.
Crossfeed	n/a	n/a	n/a	n/a	n/a	n/a
Workhead RPM	n/a	100 rpm	100 rpm	100 rpm	100 rpm	100 rpm
Coolant type	Buehler Water Sol.	Buehler Water Sol.	Buehler Water Sol.	Buehler Water Sol.	Buehler Water Sol.	Buehler Water Sol.
No. of Sparkouts	n/a	2	5	n/a	2	10
Oper.starting Dim.	1.0x2.250x8.	.530x.530x8.0	.525 x 8"	.5118 x8.0	.5118 x 1.550	.5118x1.5354
Oper. finishing Dim.	.530x.530x8.	.525 X 8.00	.5118x8.0	.5118 x 1.550	.5118x1.5354	.5118x1.5354
Surf. Fin. RA / RQ	n/a	n/a	n/a	n/a	n/a	n/a
Inspection comments	4 pcs. 8" long per billet	machined from square to round			used side of wheel to machine lenght	total infeed .025

Comments In all machining operations the Buehler Water Soluble coolant has been filtered with a Darenth Filteration system using a 5-15 micron filteration paper.

Specimen #'s machined with this process =27

3-1	4-1	4-4	6-1	6-6	7-1	8-1	8-6
	4-2	4-5	6-2	6-8	7-2	8-2	8-7
	4-3	4-6	6-3		7-3	8-3	8-8
			6-4		7-4	8-4	8-9
MED. GRIT MACH. CIRC. DIR. WITH PROCESS E WHEEL						8-5	8-10

CERAMIC MACHINING PROCEDURE #4

Specimen type Compr. Spec. **Job** Navy **Charge #** 3470-0412 **Material** Alumina AL-600

Specimen#	REFER BOTTOM		**Manufacturer** Wesgo			
Operation	Slice Billet	Rough OD	Finish OD	Rough lenght	Finish Lenght	chamfer ends
Date Oper. Finished						
Machine	Harig NC	Jungner	Jungner	Jungner	Jungner	Jungner
Operator	Jenkins	Jenkins	Jenkins	Jenkins	Jenkins	Jenkins
Tool or Wheel type	8"x .035 Resin 100 100%	8" x .5 Resin 320 150%	8" x .5 Resin 320 150%	8"x .035 Resin 100 100%	5"cupwheel Resin 320 copperdyne	8" x .5 Resin 320 150%
Downfeed or Infeed	.0005	.0002	.0002	.001	.001	.0002
Wheel speed	3400 rpm	3400 rpm	3400 rpm	3400 rpm	3400 rpm	3400 rpm
S.F.P.M.	7125	7125	7125	7125	4454	7125
Wheel or Tool Pos. Machining Direction	Wh. parallel longitudinal	Wh. perp. longitudinal	Wh. perp. longitudinal	Wh. perp. longitudinal	Wh. perp. traverse	part on 45* traverse
Wheel/Part Direction	Wh. CW	opposite	opposite	opposite	opposite	opposite
Table/traverse speed	50 in / min.	40 in / min.	20 in / min.	100 in / min	50 in / min.	20 in / min.
Crossfeed	n/a	n/a	n/a	n/a	n/a	n/a
Workhead RPM	n/a	100 rpm	100 rpm	100 rpm	100 rpm	100 rpm
Coolant type	Buehler Water Sol.	Buehler Water Sol.	Buehler Water Sol.	Buehler Water Sol.	Buehler Water Sol.	Buehler Water Sol.
No. of Sparkouts	n/a	2	5	n/a	2	10
Oper.starting Dim.	1.0x2.250x8.	.530x.530x8.0	.525 x 8"	.5118 x8.0	.5118 x 1.550	.5118x1.5354
Oper. finishing Dim.	.530x.530x8.	.525 X 8.00	.5118x8.0	.5118 x 1.550	.5118x1.5354	.5118x1.5354
Surf. Fin. RA / RQ	n/a	n/a	n/a	n/a	n/a	n/a
Inspection comments	4 pcs. 8" long per billet	machined from square to round				total infeed .025

Comments In all machining operations the Buehler Water Soluble coolant has been filtered with a Darenth Filteration system using a 5-15 micron filteration paper.

Total number of specimens = 16

Specimen #'s machined with this process

2-1	3-6	5-4	6-5	7-10	8-15
2-2	3-7	5-5	6-9	7-11	
	3-8	5-6	6-10		
		5-7	6-11		

MED. GRIT MACH. CIRC. DIRECT.

NOTE 2-2,5-6 & 6-10 DEFECTED

CERAMIC MACHINING PROCEDURE #5

Specimen type Compr. Spec. **Job** Navy **Charge #** 3470-0412 **Material** Alumina AL-600

Specimen#	Multiple		**Manufacturer** Wesgo			
Operation	Slice Billet	Rough OD	Finish OD	Rough lenght	Finish Lenght	chamfer ends
Date Oper. Finished			3-11-93	3-17-93	3-18-93	3-18-93
Machine	Harig NC	Jungner	Monarch	Harig NC	Monarch	Monarch
Operator	Jenkins	Jenkins	O'Rourke	O'Rourke	O'Rourke	O'Rourke
Tool or Wheel type	8"x .035 Resin 100 100%	8" x .5 Resin 320 150%	Diasil button tool	6" x .035 Resin 100 100%	Diasil button tool	Diasil button tool
Downfeed or Infeed	.0005	.0002	note bottom	.003	.002-.001	.001
Wheel speed	3400 rpm	3400 rpm	n/a	3400 rpm	n/a	n/a
S.F.P.M.	5350	7200	160 spec.	5300	160 spec.	160 spec.
Wheel or Tool Pos. Machining Direction	Parallel longitudinal	wheel perp longitudinal	wheel perp longitudinal	wheel perp Down	tool perp. traverse	tool on 45* traverse
Wheel/Part Direction	wh. CW	opposite	Part CCW	wh. CW	Part CCW	Part CW
Table/traverse speed	50 in / min.	40 in / min.	1.6 in/min.	100 in / min	1.6 in/min.	1.6 in/min.
Crossfeed	n/a	n/a	n/a	n/a	n/a	n/a
Workhead RPM	n/a	100 rpm	1200 rpm	n/a	1200	1200
Coolant type	Buehler Water Sol.	Buehler Water Sol.	Buehler Water Sol.	Buehler Water Sol.	Buehler Water Sol.	Buehler Water Sol.
No. of Sparkouts	n/a	2	0	n/a	0	0
Oper.starting Dim.	1.0x2.250x8.	.530x.530x8.0	.525 x 8"	.5118 x8.0	.5118 x 1.542	sharp corner
Oper. finishing Dim.	.530x.530x8.	.525 X 8.00	.5118x8.0	.5118 x 1.542	.5118x1.5354	45* X .020
Surf. Fin. RA / RQ	n/a	n/a	n/a	n/a	n/a	n/a
Inspection comments	4 pcs. 8" long per billet	machined from square to round				4-7 & 7-5 edges chip

Comments In all machining operations the Buehler Water Soluble coolant has been filtered with a Darenth Filteration system using a 5-15 micron filteration paper.
Specimens machined with Diasil button tool. Total number of specimens = 10
Specimen #'s machined with this process. 2-3 4-7 5-1 8-16 7-5
2-4 4-8 5-12 8-17 7-6
Note * infeed .004 from .525 OD to .517, .002 from .517 OD to .513, .001 from .513 to .5118

DIASIL MACHINED

CERAMIC MACHINING PROCEDURE #6

Specimen type Compr. Spec. **Job** Navy **Charge #** 3470-0412 **Material** Alumina AL-600

Specimen#	Billets 3,4,5,6,7,8	**Manufacturer**	Wesgo			
Operation	Slice Billet	Rough OD	Finish OD	Rough lenght	Finish Lenght	chamfer ends
Date Oper. Finished		3/2/93	3/11/93	3/17/93	3/22/93	
Machine	Harig NC	Jungner	Jungner	Jungner	Harig NC	Jungner
Operator	Jenkins	Jenkins	Jenkins	Jenkins	O'Rourke	Jenkins
Tool or Wheel type	8"x .035 Resin 100 100%	8" x .5 Resin 320 150%	8" x .5 Resin 320 150%	8"x .035 Resin 100 100%	8" x .5 Resin 320 150%	8" x .5 Resin 320 150%
Downfeed or Infeed	.0005	.0002	.0002	.001	.0002	.0002
Wheel speed	3400 rpm	3400 rpm	3400 rpm	3400 rpm	3400 rpm	3400 rpm
S.F.P.M.	7125	7125	7125	7125	7125	7125
Wheel or Tool Pos. Machining Direction	Wh.Parallel longitudinal	Wh. Perp. longitudinal	Wh. Perp. longitudinal	Wh. Perp. longitudinal	Wh. perp to end perp. to lgt.	part on 45* traverse
Wheel/Part Direction	Wh. CW	opposite	opposite	opposite	Wh. CW	opposite
Table/traverse speed	50 in / min.	40 in / min.	20 in / min.	100 in / min	100 in/min.	20 in / min.
Crossfeed	n/a	n/a	n/a	n/a	.0653	n/a
Workhead RPM	n/a	100 rpm	100 rpm	100 rpm	n/a	100 rpm
Coolant type	Buehler Water Sol.	Buehler Water Sol.	Buehler Water Sol.	Buehler Water Sol.	Buehler Water Sol.	Buehler Water Sol.
No. of Sparkouts	n/a	2	5	n/a	10	10
Oper.starting Dim.	1.0x2.250x8.	.530x.530x8.0	.525 x 8"	.5118 x8.0	.5118 x 1.550	sharp corner
Oper. finishing Dim.	.530x.530x8.	.525 X 8.00	.5118x8.0	.5118 x 1.550	.5118x1.5354	45* x .020
Surf. Fin. RA / RQ	n/a	n/a	n/a	n/a	n/a	n/a
Inspection comments	4 pcs. 8" long per billet	machined from square to round			machined in V-block set-up.	total infeed .025

Comments In all machining operations the Buehler Water Soluble coolant has been filtered with a Darenth Filteration system using a 5-15 micron filteration paper.

Total number of specimens = 24 Specimen #'s machined with this process

0-0	3-2	4-7	5-2	6-7	7-7	7-14	8-11	CL-1
	3-3	4-8	5-3	6-8	7-8		8-12	
	3-4	4-9	5-11		7-9		8-13	
	3-5	4-10			7-13		8-14	

MED. GRIT ENDS MACH. UNIDIR. #3-2 & 3-3 NOT FINISHED

CERAMIC MACHINING PROCEDURE #7

Specimen type MOR BAR **Job** Navy **Charge #** 3470-0412 **Material** Alumina AL600

Specimen#	7B		**Manufacturer** WESGO			
Operation	Slice Billet	slice.130 dim.	grind .157	Grind .118	Chamfer edges	
Date Oper. Finished	3/26/93	4/8/93	3/30/93	4/14/934		
Machine	Harig CNC	Harig nc	Harig CNC	Harig NC	Harig NC	
Operator	Shelton	ORourke	Shelton	ORourke	O'Rourke	
Tool or Wheel type	6"x.035 Resin 100 100%	6"x.035 Resin 100 100%	6"x.500 Resin 120 100%	6"x.500 Resin 120 100%	6" x .500 Resin 120 100%	
Downfeed or Infeed	.0005	.002	.002	.002	.002	
Wheel speed	3400	3400	6050	3400	3400	
S.F.P.M.	5350	5350	9500	7500	7500	
Wheel or Tool Pos. Machining Direction	Wh.Parallel longitudinal	Wh.Parallel longitudinal	Wh.Parallel longitudinal	Wh.Parallel longitudinal	Wh.Parallel longitudinal	
Wheel/Part Direction	Wh. CW	Wh. CW	Wh. CW	Wh. CW	Wh. CW	
Table/traverse speed	200 in/min	100in/min	360 in/min	100 in/min	100 in/min	
Crossfeed	0	0	.050	.050	n/a	
Workhead RPM	n/a	n/a	n/a	n/a	n/a	
Coolant type	Buehler Water Sol.	Buehler Water Sol.	Buehler Water Sol.	Buehler Water Sol.	Buehler Water Sol.	
No. of Sparkouts	0	0	5	10	10	
Oper.starting Dim.	2.25x4.0x.197	2.25x4x.157	.170 thick	.130	sharpcorner	
Oper. finishing Dim.	1.2x1.2x.197	2.25x.157x.130	.157 thick	.118	45°x0.007	
Surf. Fin. RA / RQ	n/a	n/a	n/a	n/a	n/a	
Inspection comments						

Comments In all machining operations the Buehler Water Soluble coolant has been filtered with a Darenth Filteration system using a 5-15 micron filteration paper.

CERAMIC MACHINING PROCEDURE #8

Specimen type MOR Bars **Job** Navy **Charge #** 3470-0412 **Material** Alumina AL-600

Specimen# 3A			**Manufacturer** Wesgo			
Operation	Slice Billet	Grind .1575 Dim	Slice Length	Slice .130 Dim	Grind .118 dim.	Chamfer edges
Date Oper. Finished						
Machine	Harig NC	Harig CNC	Harig NC	Harig NC	Harig NC	Harig NC
Operator	Shelton	Shelton	O'Rourke	O'Rourke	O'Rourke	O'Rourke
Tool or Wheel type	8" X .035 Resin 100 100%	8" X .500 Resin 320 150%	8" X .035 Resin 100 100%	8" X .035 Resin 100 100%	6" x .125 Resin 240 100%	6" x .125 Resin 240 100%
Downfeed or Infeed	.0005	.0002	.003	.003	.0005	.005
Wheel speed	3400 Rpm	3600 Rpm	3400 Rpm	3400 Rpm	3400 Rpm	3400 Rpm
S.F.P.M.	5350	7550	7200	7200	5300	5300
Wheel or Tool Pos. Machining Direction	Wh. parallel longitudinal	Wh. parallel longitudinal	Wh. perp. traverse	Wh. parallel longitudinal	Wh. parallel longitudinal	Wh. parallel longitudinal
Wheel/Part Direction	Wh. CW	Wh. CW	Wh. CW	Wh. CW	Wh. CW	Wh. CW
Table/traverse speed	200in./min.	200in. /min.	100in./min.	100in./min.	100in./min.	100in./min.
Crossfeed	n/a	.050	n/a	n/a	.030	n/a
Workhead RPM	n/a	n/a	n/a	n/a	n/a	n/a
Coolant type	Buehler water sol.	Buehler water sol.	Buehler water sol.	Buehler water sol.	Buehler water sol.	Buehler water sol.
No. of Sparkouts	0	3	0	0	10	10
Oper.starting Dim.	2.25x1.0x8"	2.25x.185x8"	2.25x.1575x4	1.968x.1575x4	1.968x.157x.13	sharp corner
Oper. finishing Dim.	2.25x.185x8"	2.25x.1575x4	1.968x.1575x4.	1.968x.157x.13	1.968x.157x.118	45*x.007
Surf. Fin. RA / RQ	n/a	n/a	n/a	n/a	n/a	n/a
Inspection comments						

Comments

CERAMIC MACHINING PROCEDURE #9

Specimen type 30x30mm **Job** Navy **Charge #** 3470-0412 **Material** Alumina AL600

Specimen#	Billet Slice 1A & Org.	**Manufacturer** WESGO				
Operation	Slice Billet	GrindEdges				
Date Oper. Finished	3/26/93	3/29/93				
Machine	Harig CNC	Harig CNC				
Operator	Shelton	Shelton				
Tool or Wheel type	6"x.035 Resin 100 100%	8"x.500 Resin 320 150%				
Downfeed or Infeed	.0005	.0002				
Wheel speed	3400	3600				
S.F.P.M.	5350	7550				
Wheel or Tool Pos. Machining Direction	Wh.Parallel longitudinal	Wh.Parallel longitudinal				
Wheel/Part Direction	Wh. CW	Wh. CW				
Table/traverse speed	200 in/min	200 in/min				
Crossfeed	0	.050				
Workhead RPM	n/a	n/a				
Coolant type	Buehler Water Sol.	Buehler Water Sol.				
No. of Sparkouts	0	3				
Oper.starting Dim.	2.25x4.0x.197	1.2x1.2x.197				
Oper. finishing Dim.	1.2x1.2x.197	1.181x1.181				
Surf. Fin. RA / RQ	n/a	n/a				
Inspection comments						

Comments In all machining operations the Buehler Water Soluble coolant has been filtered with a Darenth Filteration system using a 5-15 micron filteration paper.

Part was sliced on one side only, opposite side is original surface with edges machined to 30x30mm.

Delivered to Tom Watkins 3/26 /93

CERAMIC MACHINING PROCEDURE #10

Specimen type Compr. Spec. **Job** Navy **Charge #** 3470-0412 **Material** Alumina AL-600

Specimen#	REFER BOTTOM		**Manufacturer** Wesgo			
Operation	Slice Billet	Rough OD	Finish OD	Rough lenght	Finish Lenght	chamfer ends
Date Oper. Finished						
Machine	Harig NC	Jungner	Jungner	Jungner	Jungner	
Operator	Jenkins	Jenkins	Jenkins	Jenkins	Jenkins	
Tool or Wheel type	8"x .035 Resin 100 100%	8" x .5 Resin 320 150%	8" x .250 Resin 80 75%	8"x .035 Resin 100 100%	6"cupwheel resin150 100%	
Downfeed or Infeed	.0005	.0002	.0002	.001	.001	
Wheel speed	3400 rpm	3400 rpm	3400 rpm	3400 rpm	3400 rpm	
S.F.P.M.	7125	7125	7125	7125	5345	
Wheel or Tool Pos. Machining Direction	Wh. parallel longitudinal	Wh. perp. longitudinal	Wh. perp. longitudinal	Wh. perp. longitudinal	Wh. perp. traverse	
Wheel/Part Direction	Wh. CW	opposite	opposite	opposite	opposite	
Table/traverse speed	50 in / min.	40 in / min.	20 in / min.	100 in / min	50 in / min.	
Crossfeed	n/a	n/a	n/a	n/a	n/a	
Workhead RPM	n/a	100 rpm	100 rpm	100 rpm	100 rpm	
Coolant type	Buehler Water Sol.	Buehler Water Sol.	Buehler Water Sol.	Buehler Water Sol.	Buehler Water Sol.	
No. of Sparkouts	n/a	2	5	n/a	2	
Oper.starting Dim.	1.0x2.250x8.	.530x.530x8.0	.525 x 8"	.5118 x8.0	.5118 x 1.550	.5118x1.5354
Oper. finishing Dim.	.530x.530x8.	.525 X 8.00	.5118x8.0	.5118 x 1.550	.5118x1.5354	.5118x1.5354
Surf. Fin. RA / RQ	n/a	n/a	n/a	n/a	n/a	n/a
Inspection comments	4 pcs. 8" long per billet	machined from square to round				total infeed .025

Comments In all machining operations the Buehler Water Soluble coolant has been filtered with a Darenth Filteration system using a 5-15 micron filteration paper.

Specimen #'s machined with this process

3-9	3-13	5-8	6-12	7-12
3-10	3-14	5-9		7-13
3-11		5-10		
3-12				

COURSE GRIND ENDS MACH. CIRC.

CERAMIC MACHINING PROCEDURE #11

Specimen type Compr. Spec. **Job** **Charge #** 3470-0412 **Material** Alumina AL-600

Specimen#	REFER BOTTOM	**Manufacturer**	Wesgo Fine Grit Grind			
Operation	Slice Billet	Rough OD	Finish OD	Rough lenght	Finish Lenght	chamfer ends
Date Oper. Finished						
Machine	Harig NC	Jungner	Jungner	Jungner	Harig	Jungner
Operator	Jenkins	Jenkins	Jenkins	Jenkins	O'Rourke	Jenkins
Tool or Wheel type	8"x .035 Resin 100 100%	8" x .5 Resin 320 150%	7" x .5 Resin12mic 100%	8"x .035 Resin 100 100%	7" x .5 Resin12mic 100%	7" x .5 Resin12mic 100%
Downfeed or Infeed	.0005	.0002	.0001	.001	.0001	.0002
Wheel speed	3400 rpm	3400 rpm	3400 rpm	3400 rpm	3400 rpm	3400 rpm
S.F.P.M.	7125	7125	6200	7125	6200	6200
Wheel or Tool Pos. Machining Direction	Wh. parallel longitudinal	Wh. perp. longitudinal	Wh. perp. longitudinal	Wh. perp. longitudinal	Wh. perp. traverse	part on 45* traverse
Wheel/Part Direction	Wh. CW	opposite	opposite	opposite	opposite	opposite
Table/traverse speed	50 in / min.	40 in / min.	20 in / min.	100 in / min	50 in / min.	20 in / min.
Crossfeed	n/a	n/a	n/a	n/a	n/a	n/a
Workhead RPM	n/a	100 rpm	100 rpm	100 rpm	100 rpm	100 rpm
Coolant type	Buehler Water Sol.	Buehler Water Sol.	Buehler Water Sol.	Buehler Water Sol.	Buehler Water Sol.	Buehler Water Sol.
No. of Sparkouts	n/a	2	5	n/a	2	10
Oper.starting Dim.	1.0x2.250x8.	.530x.530x8.0	.525 x 8"	.5118 x8.0	.5118 x 1.550	.5118x1.5354
Oper. finishing Dim.	.530x.530x8.	.525 X 8.00	.5118x8.0	.5118 x 1.550	.5118x1.5354	.5118x1.5354
Surf. Fin. RA / RQ	n/a	n/a	n/a	n/a	n/a	n/a
Inspection comments	4 pcs. 8" long per billet	machined from square to round				total infeed .025

Comments In all machining operations the Buehler Water Soluble coolant has been filtered with a Darenth Filteration system using a 5-15 micron filteration paper.

Specimen #'s machined with this process =14

1-1	1-5	2-5	2-9
1-2	1-6	2-6 CHIPPED	2-10
1-3	1-7	2-7	
1-4	1-8	2-8	

FINE GRIND ENDS MACH UNIDIR.

CERAMIC MACHINING PROCEDURE #12

Specimen type Compr. Spec. **Job** Navy **Charge #** 3470-0412 **Material** Alumina AL-600

Specimen#	REFER BOTTOM		**Manufacturer** Wesgo			
Operation	Slice Billet	Rough OD	Finish OD	Rough lenght	Finish Lenght	chamfer ends
Date Oper. Finished						
Machine	Harig NC	Jungner	Jungner	Jungner	Harig NC	
Operator	Jenkins	Jenkins	Jenkins	Jenkins	O'ROURKE	
Tool or Wheel type	8"x .035 Resin 100 100%	8" x .5 Resin 320 150%	8" x .5 Resin 320 150%	8"x .035 Resin 100 100%	8"x .035 Resin 100 100%	
Downfeed or Infeed	.0005	.0002	.0002	.001	.0005	
Wheel speed	3400 rpm	3400 rpm	3400 rpm	3400 rpm	3400 rpm	
S.F.P.M.	7125	7125	7125	7125	7125	
Wheel or Tool Pos. Machining Direction	Wh. parallel longitudinal	Wh. perp. longitudinal	Wh. perp. longitudinal	Wh. perp. longitudinal	Wh. perp. traverse	
Wheel/Part Direction	Wh. CW	opposite	opposite	opposite	opposite	
Table/traverse speed	50 in / min.	40 in / min.	20 in / min.	100 in / min	50 in / min.	
Crossfeed	n/a	n/a	n/a	n/a	n/a	
Workhead RPM	n/a	100 rpm	100 rpm	100 rpm	100 rpm	
Coolant type	Buehler Water Sol.	Buehler Water Sol.	Buehler Water Sol.	Buehler Water Sol.	Buehler Water Sol.	
No. of Sparkouts	n/a	2	5	n/a	2	
Oper.starting Dim.	1.0x2.250x8.	.530x.530x8.0	.525 x 8"	.5118 x8.0	.5118 x 1.550	
Oper. finishing Dim.	.530x.530x8.	.525 X 8.00	.5118x8.0	.5118 x 1.550	.5118x1.483	
Surf. Fin. RA / RQ	n/a	n/a	n/a	n/a	n/a	
Inspection comments	4 pcs. 8" long per billet	machined from square to round				

Comments In all machining operations the Buehler Water Soluble coolant has been filtered with a Darenth Filteration system using a 5-15 micron filteration paper.

Total number of specimens = 6

Specimen #'s machined with this process

4-11 4-14
4-12 4-15
4-13 4-16

AS SAWN

APPENDIX B
MECHANICAL TESTING DATA

MOR BARS

Data for all of the specimens tested are presented in the following tables.

Table B1. Data Summary for Flexure Strength Measurements.

Specimen Number	Grinding Procedure	Material	Width (mm)	Height (mm)	Strength (ksi)	Strength (MPa)
1B1-10	1	WESGO AL-600	4.000	2.994	43.93	302.88
1B1-2	1	WESGO AL-600	4.006	3.001	47.76	329.29
1B1-5	1	WESGO AL-600	4.007	3.004	48.01	331.04
1B1-13	1	WESGO AL-600	4.007	2.988	48.77	336.27
1B1-16	1	WESGO AL-600	4.007	2.995	50.36	347.22
1B1-4	1	WESGO AL-600	4.003	2.992	50.88	350.77
1B1-11	1	WESGO AL-600	4.006	2.983	50.90	350.95
1B1-18	1	WESGO AL-600	4.008	2.967	51.55	355.41
1B1-14	1	WESGO AL-600	4.009	2.978	51.77	356.92
1B1-7	1	WESGO AL-600	4.006	3.000	52.26	360.29
1B1-6	1	WESGO AL-600	4.009	2.999	52.61	362.76
1B1-17	1	WESGO AL-600	4.006	2.994	52.95	365.08
1B1-15	1	WESGO AL-600	4.007	3.002	53.14	366.37
1B1-1	1	WESGO AL-600	4.008	3.001	53.52	369.02
1B1-19	1	WESGO AL-600	4.006	3.007	53.82	371.04
1B1-12	1	WESGO AL-600	4.007	2.987	53.92	371.74
1B1-20	1	WESGO AL-600	4.006	2.993	54.56	376.19
1B1-9	1	WESGO AL-600	4.007	2.989	54.82	377.94
1B1-3	1	WESGO AL-600	4.008	2.997	55.72	384.17
1B1-8	1	WESGO AL-600	4.007	2.976	56.89	392.24
2B2-19	2	WESGO AL-600	4.010	2.981	36.51	251.72
2B2-7	2	WESGO AL-600	4.014	2.998	38.83	267.75
2B2-12	2	WESGO AL-600	4.013	2.999	40.14	276.79
2B2-13	2	WESGO AL-600	4.014	2.988	40.92	282.11
2B2-11	2	WESGO AL-600	4.011	3.009	41.10	283.35
2B2-14	2	WESGO AL-600	4.014	2.993	44.29	305.36
2B2-10	2	WESGO AL-600	4.014	2.989	45.38	312.87
2B2-17	2	WESGO AL-600	4.013	3.001	47.07	324.56
2B2-15	2	WESGO AL-600	4.012	2.990	48.04	331.22
2B2-9	2	WESGO AL-600	4.014	2.986	48.27	332.78
2B2-1	2	WESGO AL-600	4.011	2.990	48.29	332.97
2B2-18	2	WESGO AL-600	4.012	3.006	48.73	335.98
2B2-6	2	WESGO AL-600	4.013	2.994	48.75	336.09
2B2-4	2	WESGO AL-600	4.016	2.981	49.50	341.29
2B2-8	2	WESGO AL-600	4.015	2.983	49.57	341.76
2B2-3	2	WESGO AL-600	4.015	2.989	49.73	342.90
2B2-2	2	WESGO AL-600	4.007	2.999	50.95	351.29
2B2-16	2	WESGO AL-600	4.014	2.999	50.98	351.50
2B2-5	2	WESGO AL-600	4.016	2.991	51.11	352.38
2B2-20	2	WESGO AL-600	4.008	3.004	51.73	356.67

Table B1. Data Summary for Flexure Strength Measurements (Continued).

Specimen Number	Grinding Procedure	Material	Width (mm)	Height (mm)	Strength (ksi)	Strength (MPa)
N7B1,2-12	7	WESGO AL-600	3.948	3.006	40.25	277.51
N7B1,2-20	7	WESGO AL-600	3.948	3.023	40.76	281.05
N7B1,2-8	7	WESGO AL-600	3.961	3.005	41.00	282.66
N7B1,2-11	7	WESGO AL-600	3.962	3.003	41.16	283.80
N7B1,2-1	7	WESGO AL-600	3.949	3.008	41.65	287.15
N7B1,2-7	7	WESGO AL-600	3.975	3.028	41.90	288.92
N7B1,2-5	7	WESGO AL-600	3.947	3.008	43.50	299.89
N7B1,2-17	7	WESGO AL-600	3.959	3.175	43.72	301.43
N7B1,2-10	7	WESGO AL-600	3.965	3.002	43.84	302.25
N7B1,2-14	7	WESGO AL-600	3.947	3.007	43.89	302.61
N7B1,2-4	7	WESGO AL-600	3.949	3.007	44.23	304.98
N7B1,2-3	7	WESGO AL-600	3.952	3.004	44.90	309.57
N7B1,2-16	7	WESGO AL-600	3.947	3.000	45.08	310.78
N7B1,2-6	7	WESGO AL-600	3.970	3.004	45.30	312.35
N7B1,2-19	7	WESGO AL-600	3.936	3.014	45.88	316.32
N7B1,2-2	7	WESGO AL-600	3.958	3.008	46.05	317.49
N7B1,2-13	7	WESGO AL-600	3.952	3.007	46.51	320.70
N7B1,2-15	7	WESGO AL-600	3.959	3.008	46.89	323.27
N7B1,2-9	7	WESGO AL-600	3.958	3.007	47.90	330.27
N7B1,2-18	7	WESGO AL-600	3.948	3.006	48.67	335.54
NTL-4	2[a]	COORS AD-94	3.983	3.007	41.80	288.22
NTL-3	2[a]	COORS AD-94	3.981	3.003	42.18	290.80
NTL-2	2[a]	COORS AD-94	3.988	2.991	42.93	295.99
NTL-18	2[a]	COORS AD-94	3.988	2.997	43.00	296.48
NTL-16	2[a]	COORS AD-94	3.983	2.989	43.04	296.76
NTL-13	2[a]	COORS AD-94	3.983	3.000	43.09	297.10
NTL-9	2[a]	COORS AD-94	3.987	2.999	43.32	298.67
NTL-11	2[a]	COORS AD-94	3.983	3.002	43.76	301.71
NTL-8	2[a]	COORS AD-94	3.987	3.003	44.29	305.38
NTL-19	2[a]	COORS AD-94	3.983	2.999	44.33	305.67
NTL-7	2[a]	COORS AD-94	3.986	2.999	44.66	307.95
NTL-15	2[a]	COORS AD-94	3.982	2.997	44.89	309.51
NTL-5	2[a]	COORS AD-94	3.986	2.997	45.33	312.55
NTL-10	2[a]	COORS AD-94	3.987	2.996	45.35	312.68
NTL-6	2[a]	COORS AD-94	3.984	3.002	45.57	314.17
NTL-17	2[a]	COORS AD-94	3.986	2.997	46.18	318.42
NTL-14	2[a]	COORS AD-94	3.982	2.979	46.67	321.75
NTL-12	2[a]	COORS AD-94	3.982	2.994	46.69	321.90
NTL-1	2[a]	COORS AD-94	3.981	3.004	47.36	326.52
NTC-4	2[b]	COORS AD-94	3.999	2.997	38.89	268.10
NTC-3	2[b]	COORS AD-94	4.000	2.969	39.74	273.97
NTC-1	2[b]	COORS AD-94	4.020	2.966	40.60	279.94
NTC-5	2[b]	COORS AD-94	3.999	2.986	42.47	292.80
NTC-2	2[b]	COORS AD-94	4.000	2.969	42.70	294.39

(a) Specimens cut from existing cylinder parallel to longitudinal axis of cylinder.
(b) Specimens cut from existing cylinder parallel to circumference of cylinder.

Table B2. Summary of Compression Specimens.

Specimen Number	Grinding Procedure	Diameter (mm)	Length (mm)	Mass (g)	Max/Min Stress Ratio (ksi)/(ksi)	Test Type
N4-1	3	13.00	38.95	19.304	130 / 13	Cyclic Loading
N4-2	3	12.99	38.98	19.292	70 / 7	Cyclic Loading
N4-3	3	13.01	38.92	19.295	115 / 11.5	Cyclic Loading
N6-2	3	13.02	39.00	19.317	130 / 13	Cyclic Loading
N6-3	3	13.01	39.00	19.342	130/13	Cyclic Loading
N7-4	3	13.00	39.05	19.336	130 / 13	Cyclic Loading
N8-1	3	13.00	39.00	19.299	100/10	Cyclic Loading
N8-2	3	13.00	39.01	19.326	120/12	Cyclic Loading
N8-6	3	13.04	39.08	19.306	120/12	Cyclic Loading
N5-1	5	13.05	38.95	19.241	70/7	Cyclic Loading[b]
N7-6	5	12.96	38.98	19.267	80/8	Cyclic Loading[b]
N8-13	5	13.02	38.98	19.264	90/9	Cyclic Loading
N7-14	6	13.06	39.05	19.361	90/9	Cyclic Loading[b]
N7-13	6	13.05	39.02	19.357	100/10	Cyclic Loading[b]
N6-8	6	13.01	39.00	19.345	120/12	Cyclic Loading[b]
N7-7	6	13.06	39.00	19.353	120/12	Cyclic Loading
N7-8	6	13.09	39.00	19.339	120/12	Cyclic Loading
N6-1	3	13.08	39.05	N/A		Strength Testing
N7-1	3	12.99	39.06	19.32		Strength Testing
N7-2	3	13.00	39.00	19.34		Strength Testing
N8-4	3	13.00	38.96	19.264		Strength Testing
N8-5	3	13.03	38.96	19.239		Strength Testing
N8-7	3	13.01	38.91	19.231		Strength Testing
N2-1	4	13.03	38.98	19.312		Strength Testing
N3-6	4	13.05	38.94	19.315		Strength Testing
N3-7	4	13.08	39.00	19.321		Strength Testing
N3-8	4	13.03	39.05	19.318		Strength Testing
N3-5	5	13.01	38.94	19.309		Strength Testing
N5-2	5	13.05	39.03	19.343		Strength Testing
N4-7	5	13.01	38.97	19.307		Strength Testing
N4-8	5	12.97	38.99	19.277		Strength Testing
N8-11	5	13.01	39.01	19.296		Strength Testing
N8-12	5	13.00	38.95	19.302		Strength Testing
N5-1	5	13.05	38.95	19.241		Strength Testing
N7-6	5	12.96	38.98	19.267		Strength Testing
N5-3	6	13.09	39.04	19.537		Strength Testing
N5-11	6	13.01	39.01	19.336		Strength Testing
N7-14	6	13.06	39.05	19.361		Strength Testing
N7-13	6	13.05	39.02	19.357		Strength Testing
N6-8	6	13.01	39.00	19.345		Strength Testing
A0-0	a	13.00	51.38	28.72		Strength Testing
A5-5	a	13.04	51.47	28.862		Strength Testing
A6-9	a	12.99	51.28	28.764		Strength Testing
A7-10	a	13.04	51.26	28.704		Strength Testing

(a) Specimens with brazed zirconia end caps.
(b) Cyclic loading terminated and specimens loaded to failure.

Table B2. Summary of Compression Specimens (Continued).

Specimen Number	Grinding Procedure	Diameter (mm)	Length (mm)	Mass (g)	Max/Min Stress Ratio (ksi)/(ksi)	Test Type
N8-8	3	13.02	38.98	19.301		Archive
N5-4	4	13.03	38.95	19.305		Archive
N7-5	5	13.05	38.99	19.275		Archive
N6-7	6	13.01	39.04	19.332		Archive
N7-7	?	13.06	39.00	19.353		Archive
N7-8	6	13.09	39.00	19.339		Archive
N7-3	3	13.01	39.04	N/A		Archive

Table B3. Summary of Compression Cyclic Load Tests.

Specimen Number	Grinding Procedure	Percent Bending	Max/Min Stress Ratio (ksi)/(ksi)	Cycles to Failure	Ti Batch Number	Ti Condition	Comments
N4-1	3	4.7	130 / 13	18990	1	As Received	
N4-2	3	8.4	70 / 7	520000	1	As Received	Test Interrupted
N4-3	3	7.6	115 / 11.5	174745	1	As Received	Test Interrupted
N6-2	3	8	130 / 13	3670	1	As Received	
N6-3	3	5.7	130/13	2448	1	As Received	Small Cracks
N6-8	3	8.6	120/12	334448	2	As Received	Test Interrupted
N7-4	3		130 / 13	13600	1	As Received	
N8-1	3	3.5	100/10	240000	1	As Received	Test Interrupted
N8-2	3	6.1	120/12	125882	1	As Received	Small Cracks
N8-6	3	2.6	120/12	0	1	Annealed Unpolished	Small Cracks During Loading
N5-1	5	6.3	70/7	271760	2	As Received	Test Interrupted
N7-6	5	8.7	80/8	379090	2	As Received	Test Interrupted
N8-13	5	8	90/9	N/A	2	As Received	Accidental Failure
N7-13	6	5.2	100/10	332860	2	As Received	Test Interrupted
N7-14	6	8.9	90/9	276235	2	As Received	Test Interrupted
N7-7	6	8.5	120/12	<50000	2	As Received	Small Cracks
N7-8	6	10.2	120/12	<50000	2	As Received	Small Cracks

Table B4. Summary of Compression Strength Tests.

Specimen Number	Grinding Procedure	Percent Bending	Strength (GPa)	Ti Batch Number	Ti Condition
N6-1	3	4.7	(a)	1	As Received
N7-1	3	N/A	1.16	No Disks	As Received
N7-2	3	N/A	1.14	No Disks	As Received
N8-4	3	7.4	0.95	1	As Received
N8-5	3	7.2	1.05	1	As Received
N8-7	3	8.9	0.58	1	Annealed & Cleaned in Acetone
N2-1	4	3.9	1.06	1	As Received
N3-6	4	7.2	1.06	1	As Received
N3-7	4	0.7	1.15	1	Annealed & Polihed
N3-8	4	4.6	0.65	2	As Received
N3-5	5	4.0	1.04	1	As Received
N5-2	5	8.0	1.08	1	As Received
N4-7	5	4.5	1.02	1	As Received
N4-8	5	9.0	1.06	1	As Received
N8-11	5	3.8	0.88	2	As Received
N8-12	5	7.7	1.08	1	Annealed & Polihed
N5-1	5	4.5	1.07	2	As Received
N7-6	5	8.7	1.02	2	As Received
N5-3	6	9.3	1.01	1	As Received
N5-11	6	2.9	1.04	1	As Received
N7-14	6	8.9	1.04	2	As Received
N7-13	6	5.2	1.04	2	As Received
N6-8	6	8.6	1.06	2	As Received
A0-0	b	21.7	1.09	2	As Received
A5-5	b	19.6	1.16	2	As Received
A6-9	b	9.1	1.15	2	As Received
A7-10	b	10.8	1.17	2	As Received

(a) Inadvertently fractured.
(b) Specimens with brazed zirconia end caps.

Table B5. Data Summary for Flexure Strength Measurements of Surface Modified Bars of Wesgo AL-600. All were machined by Procedure 1, from billet Series 1B.

Specimen Code	Treatment	Width (mm)	Height (mm)	Strength (ksi)	Strength (MPa)
AP-1	Annealed	4.014	3.003	41.35	285.10
AP-2	Annealed	4.015	3.006	44.86	309.26
AP-3	Annealed	4.013	2.998	45.12	311.07
AP-4	Annealed	4.012	2.997	45.04	310.52
AP-5	Annealed	4.012	2.996	47.24	325.73
A-I	Ion-Implanted	4.014	3.016	51.24	353.30
B-I	Ion-Implanted	4.009	3.007	51.61	355.87
B1-I	Ion-Implanted	4.015	3.005	50.77	350.02
AP-6	Ion-Exchanged	4.001	2.986	52.81	364.13
AP-7	Ion-Exchanged	4.014	2.997	46.22	318.69
AP-8	Ion-Exchanged	4.008	2.999	42.61	293.78

Photographs of the mechanical testing equipment are presented in Figs. B1 through B4. Fig. B1 shows the test fixture for the four-point bending MOR test. Fig. B2 shows the fixture in the load transfer device on the Instron test machine. Electrical output wires are for the strain gages. Fig. B3 shows the test setup for compressive strength and compressive fatigue testing, while Fig. B4 shows detail of the cylindrical specimen. Again, the wires are for the strain gages.

Fig. B1

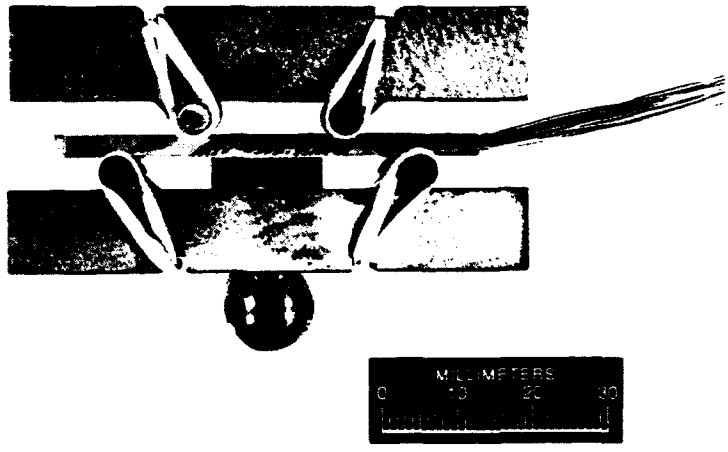

Fig. B2

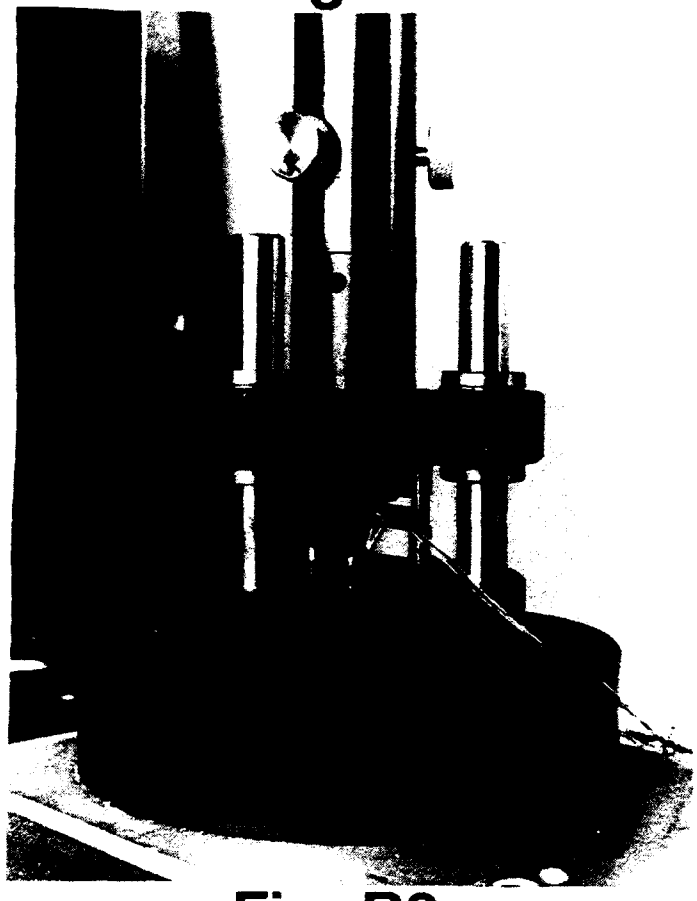

Fig. B3

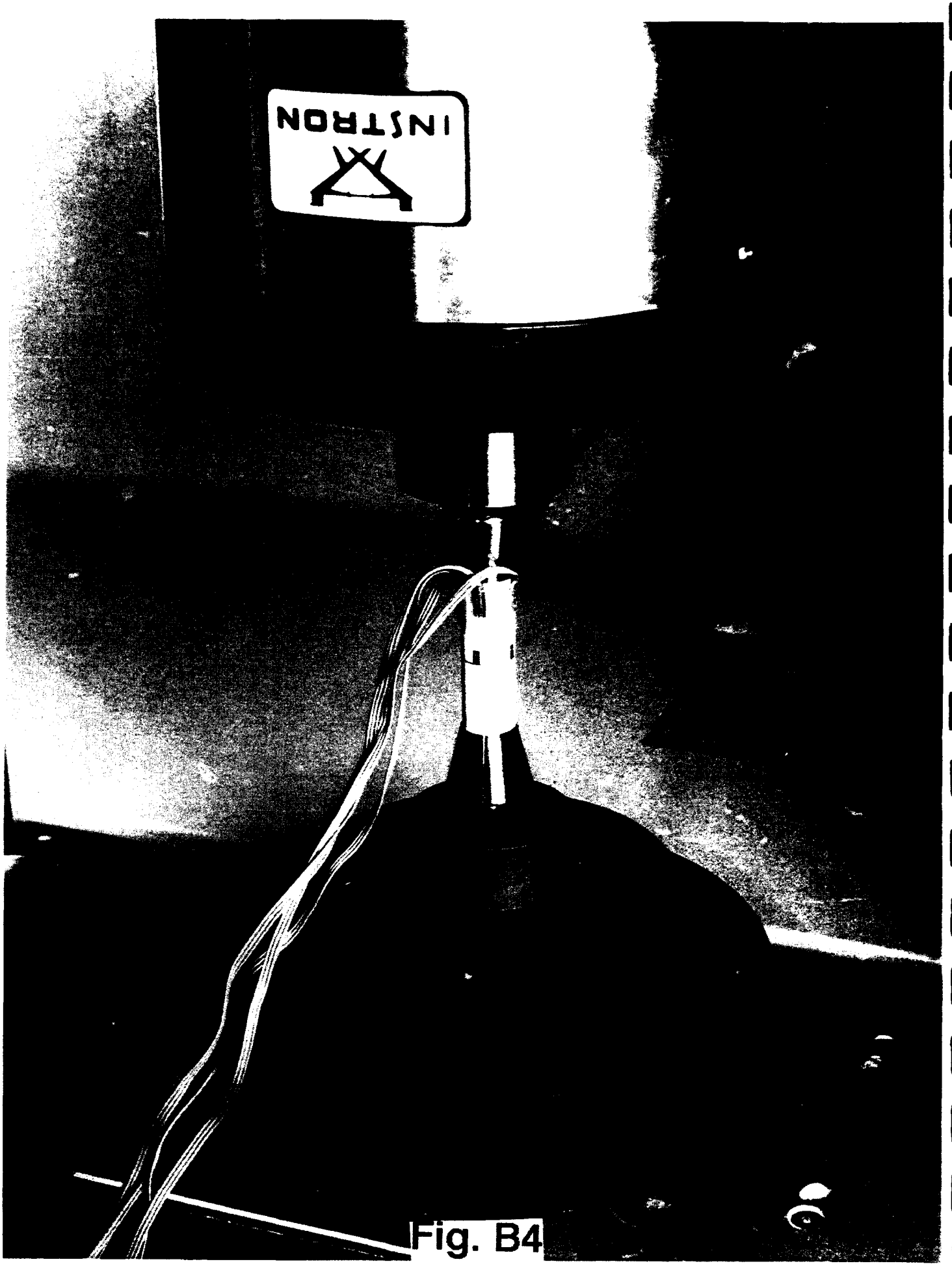

Fig. B4

REPORT DOCUMENTATION PAGE

Form Approved
OMB No. 0704-0188

1. AGENCY USE ONLY *(Leave blank)*	2. REPORT DATE	3. REPORT TYPE AND DATES COVERED
	November 1993	Final

4. TITLE AND SUBTITLE
EFFECT OF SURFACE CONDITION ON STRENGTH AND FATIGUE BEHAVIOR OF ALUMINA CERAMIC

5. FUNDING NUMBERS
C: N66001-92-M-P00120
PE: 0603713N
WU: DN302232

6. AUTHOR(S)

7. PERFORMING ORGANIZATION NAME(S) AND ADDRESS(ES)
Naval Command, Control and Ocean Surveillance Center (NCCOSC)
RDT&E Division
San Diego, CA 92152-5001

8. PERFORMING ORGANIZATION REPORT NUMBER
TD 2584

9. SPONSORING/MONITORING AGENCY NAME(S) AND ADDRESS(ES)
Naval Sea Systems Command
Washington, DC 20362

10. SPONSORING/MONITORING AGENCY REPORT NUMBER

11. SUPPLEMENTARY NOTES

12a. DISTRIBUTION/AVAILABILITY STATEMENT
Approved for public release; distribution is unlimited.

12b. DISTRIBUTION CODE

13. ABSTRACT *(Maximum 200 words)*

The United States Navy is developing deep-water submersible vessels and, in an effort to attain the appropriate strength and buoyancy characteristics, is investigating the suitability of ceramics. The vessels typically consist of cylindrical sections and hemispherical end caps of a ceramic such as aluminum oxide (alumina), which are joined together via metallic rings made of a titanium alloy. Tests of such vessels have shown that fatigue cracks may arise in the alumina during submergence-emergence cycles, which ultimately lead to failure of the vessel.

This document presents results from a one-year program designed to develop a fatigue-crack-growth resistant interface between the alumina cylinder sections and the titanium alloy rings.

14. SUBJECT TERMS
ceramics
external pressure housing
ocean engineer

15. NUMBER OF PAGES
84

16. PRICE CODE

17. SECURITY CLASSIFICATION OF REPORT	18. SECURITY CLASSIFICATION OF THIS PAGE	19. SECURITY CLASSIFICATION OF ABSTRACT	20. LIMITATION OF ABSTRACT
UNCLASSIFIED	UNCLASSIFIED	UNCLASSIFIED	SAME AS REPORT

21a. NAME OF RESPONSIBLE INDIVIDUAL	21b. TELEPHONE *(include Area Code)*	21c. OFFICE SYMBOL
R. Kurkchubasche, COTR	(619) 553-1949	Code 564